Demonstrating lower polluting solutions for sustainable airports across Europe

GRANT AGREEMENT NO. 101036996

START DATE 01.01.2022 END DATE 31.12.2025

Deliverable 7.2

Airside UFP Mitigation By Using a Water Spray System

Public

DUE DATE OF DELIVERABLE: 31/07/2024

SUBMISSION DATE 11/09/2024

REVISION	ORGANIZATION & PERSON	DATE
Written by	NLR, Timothy van der Duim NLR, Richard Rong NLR, Rui Roosien RSG, Ece Rousian RSG, Yannick Enting	01/07/2024
Checked by	NLR, Theo van Veen	20/07/2024
Approved by	SNBV, Fokko Kroesen	28/08/2024

This project has received funding from the European Union's Horizon 2020 research and innovation programme under grant agreement No. 101036996.

I. DELIVERABLE INFORMATION

Deliverable Number	7.2
Deliverable Title	UFP Reduction By Using Water spray system – Test Methodology and Results
Work Package	WP 7.1
Date of Issue	11/09/2024
Version Number	V3
Nature of Deliverable	Report
Dissemination Level (Public / Confidential)	Public

Author(s)	T.Y. van der Duim, R. Rong, R.J. Roosien, E. Rousian, T van Veen, Y.G. Enting
Keywords	UFP, mitigation, water droplets

Abstract

Deliverable 7.2 reviews and summarizes findings from experiments at Amsterdam Airport Schiphol, focusing on a demonstrator developed under WP7.1. This demonstrator tested whether a 'screen of water droplets' could reduce Ultra Fine Particles (UFP) concentrations behind a running aircraft engine. The test setup included a 4x2 meter metal frame with over 200 nozzles, targeting UFP emissions from a Cessna Citation II jet. While the system increased particle size downstream, the reduction in UFP concentrations was below the targeted 15% and highly dependent on wind direction. The study concludes that this mitigation method is not operationally feasible due to UFP complexity. Future efforts will focus on continuous measurement and data analysis to better understand UFP behavior and develop effective mitigation strategies in airport environments.

II. DOCUMENT HISTORY

Date	Version	Modified by	Remarks
01-03-2024	1	R. Rong, T.Y. van der Duim	First concept, unpolished & unfinished
27-05-2024	2	Y.G. Enting & E. Rousian	Review
17-06-2024	3	R.J. Roosien, T.Y. van der Duim	Final draft

III. TABLE OF CONTENTS

IV. LIST OF FIGURES

V. LIST OF TABLES

VI. LIST OF ACRONYMS

Acronym	Meaning
µm	Micrometer
APU	Auxiliary power unit
°C	Celsius
CO_2	Carbon dioxide
D10	Performance metric for which 10% of the droplets are finer than the stated diameter, geometric mean
D32	Also known as Sauter mean diameter. Performance metric of the droplet diameter that has the same volume to surface area ratio as the entire spray
EHRD	ICAO code for Rotterdam The Hague Airport
EHTW	ICAO code for Twente Airport
FMPS	Fast Mobility Particle Sizer Spectrometer model 3091 by TSI
GA	General Assembly
HEPA	High-efficiency particulate air
KDE	Kernel density estimate
KLM	Koninklijke Nederlandse Luchtvaartmaatschappij
KOM	Kick Off Meeting
LCS	Low-Cost Sensors
LDSA	Lung-Deposited Surface Area
LDSA	Lung-deposited surface area
NLR	Netherlands Aerospace Centre
nm	Nanometer
NO_X	Nitrous oxide
nvPM	Non-volatile PM
PCA	Principal Component Analysis
PM	Particulate Matter
PM10	PM with a diameter <10 micrometer

PM2.5	PM with a diameter <2.5 micrometer
RH	Relative humidity
RIVM	Rijksinstituut voor Volksgezondheid en Milieu
RSG	Royal Schiphol Group
SNBV	Schiphol Nederland B.V.
TNO	Stichting voor Toegepast Natuurkundig Onderzoek
TPM	Total PM
UFP	Ultra Fine Particles
VOC	Volatile organic compound
vPM	Volatile PM
WHO	World Health Organisation
WP	Work Package

1 Executive Summary

Deliverable 7.2 reviews, evaluates, and summarizes the findings from previous experiments conducted at Amsterdam Airport Schiphol over a specified period (0-30 months of the project).

Building upon these findings, demonstrator for WP7.1 is developed, aiming to test whether a ‘screen of water droplets’ can reduce Ultra Fine Particles (UFP) concentrations behind a running aircraft engine, for example during engine start-up. The demonstrator consisted of metal frame of 4 meters wide and 2 meters high with more than 200 nozzles producing a volume filled with fine water droplets (8 micrometre, D10[1]). The emission source of UFP was the left engine of a Cessna Citation II, a typical light business jet seating 6 to 8 passengers.

The test showed an effect on the mean particle size downstream of the water spray system (increased particle size downstream, compared with the upstream particles), the reduction in UFP concentration (<0.1 micrometre) was smaller than the ~15% reduction that was aimed for. Also the observed reduction proved highly dependent on wind direction.

We conclude that mitigation with the water spray system demonstrated in WP7.1 is not operational feasible due to the complexity of UFP and the mitigation set-up.

The study has unveiled several uncertainties regarding UFP behaviour and influencing factors. While existing research provides valuable insights, critical gaps persist. Numerous variables impact UFP behaviour, yet their precise effects remain unclear. This complexity underscores a significant gap in our comprehension, especially concerning the real-world operational environment of an airport.

RSG has put effort into establishing a continuous measurement network within airport operations. By concentrating on continuous measurement and detailed data analysis in the next stage of our demo development (see next report D7.3), RSG aims to uncover the nuances of UFP behaviour and develop strategies for effective mitigation. This approach will enable to address the complexities and challenges identified in our experiments, ultimately leading to improved air quality management at the airport.

[1] Performance metric for which 10% of the droplets are finer than the stated diameter, geometric mean

2 Introduction

2.1 Problem statement

Adverse health effects, especially among platform workers, due to UFP concentrations from aircraft engines among other sources of UFP are an area of concern. At the moment of writing, the scale of the problem, the causal relations, and effective means for mitigation are all not sufficiently understood or implementable.

2.2 Context within TULIPS

TULIPS is a consortium that will develop innovations that facilitate the transition to mobility with low-carbon emissions and enhance sustainability at airports for the next four years, supported by the EU with €25 million in funding. The TULIPS project has started in January 2022 and lasts until December 2025. The collaboration of frontrunning airports, airlines, knowledge institutes and industrial partners in this unique European consortium made it possible to contribute significantly to sustainable aviation, on top of current contributions and actions planned.

Collaboration by four very different airports, with the input from the broad coalition of partners, will allow the impact of the solutions on the European climate targets to become apparent. Successful demonstration of specific actions to accelerate sustainability in different scenarios will showcase these innovations and how they can be implemented throughout Europe. The outcomes of the project are expected to contribute significantly to the decarbonisation and sustainability of the aviation sector and accelerate the implementation of innovative and sustainable technologies to reduce emissions at airports. Amsterdam Airport Schiphol will be the proving ground for 17 demonstrator projects that result from the collaboration.

WP7.1 is to specifically assesses the mitigation of UFP at airports. The overall goal is to test and demonstrate the potential of a ‘screen of water droplets’ to significantly (15% reduction) reduce UFP concentrations behind a running aircraft engine in an airport environment, for example during engine start-up.

The TULIPS program is structured into various Work Packages (WPs). WP7.1 focuses on Airside UFP Mitigation over a timeline of 48 months. The project is led by SNBV with participation by NLR. The objectives and tasks are as follows:

- Specify and build a water spray prototype led by SNBV
- Validation measurements using the water spray prototype led by NLR
- Assessment of conditions affecting implementation including local air quality measurements, operational and economic considerations led by SNBV

The work packages have various deliverables (D). Deliverable 7.2 is the "Report of Current Airside UFP Levels and Ionized Mist First Results," scheduled for completion by month 30 (M30). This deliverable includes:

- Assessment of Airborne Ultrafine Particles (UFP): SNBV will conduct an assessment of UFP levels at Amsterdam Airport Schiphol.
- Airside UFP Mitigation By Using a Water Spray System: The report will provide the evaluation, test methodology and results.

2.3 Readers guide

Section 3 starts with an overview of relevant literature about guidelines for UFP monitoring, UFP and aviation and the use of water to lower UFP concentrations. Section 4 then gives an overview of recent efforts at Amsterdam Airport Schiphol to improve the local air quality at the airport. Section 5 thoroughly describes the methodology of the test and the tools that were used. Results are then described and discussed in section 6 for both the main experiment and the two so-called pre-tests. Finally, section 7 draws the conclusions with respect to the main goals of WP7.1 and provides recommendations for further work.

3 Assessment of airborne UFP at Royal Schiphol Group

This section provides an overview of what we know through the measurements and experiments performed since 2022 at Royal Schiphol Group.

3.1 UFP measurements

Measurements and experiments on UFP at Royal Schiphol Group have took place since 2015. Since the start of this project in 2022, 7 measurements and experiments have taken place that bring insights for a developing an understanding of UFP concentrations. This chapter provides an overview of these measurements and experiments. Each learning served as a foundation for subsequent ones.

3.2 Measurements and experiments at Royal Schiphol Group

As of 2022 a variety of measurements and experiments have been performed to gain insight in UFP.

- 2022 Amsterdam Airport Schiphol: Droplet Screen Experiment

During 1 day in March, different set-ups in 3 different situations with water droplets at Amsterdam Airport Schiphol were tested to find out if water droplets can mitigate UFP levels in the air. A water spray cannon was used for 'full blast' engine settings and a spray wall of water was used for engine start & ground idle settings. They were directed at or placed directly behind a plane. The test setting was performed with a Boeing 737-86J from Corendon. Situations with airplane engines running at 80% or 40% of their capacity were tested.

- 2022 TNO Eindhoven Airport: UFP Concentrations

For a period of 4 weeks during April & May, at 2 locations a set with UFP sensors have been put in place to measure UFP concentrations. The locations are situated at the so called expected worse case points; between the platforms and close to the taxiway. The measurements were constant for 24 hours per day with airplane movements between 7:00 AM and 7:00 PM. From these data, the average values over 8 hours were used in the analysis. Black carbon measurements, with an, aethalometer AE33 (Magee Scientific), were performed as well, to distinguish between the effects of ground traffic and air traffic.

- TNO Rotterdam Airport: UFP Concentrations

For a period of 4 weeks during July 2022, at 2 locations a set with UFP sensors have been put in place to measure UFP concentrations. The locations are situated between the platforms and close to the taxiway, the so called expected worse case points. Different UFP sensors were used to compare the results and useability of the different sensors. PM levels were measured to find potential proxies for UFP measurements. Black carbon and sulfur dioxide measurements were performed as well.

- 2022 Amsterdam Airport Schiphol: Overpressure Experiment

The differences in UFP concentrations for an inside environment at Amsterdam Airport Schiphol were measured (fire brigade building). These measurements took place over a period of 3 weeks and were repeated 5 times to get indicative results. After these measurements of the concentration, the UFP in the inside environment was filtered. Filtering took place by machine which operates on a clustering principle, where particles larger than 100 nm are grouped together. These clustered particles are then filtered out with a HEPA filter. As a result of this change, the inside pressure increased and insights were gathered to see how that reflected in a reduction of new UFP entering the building. Humidity was recorded per day to get indications for the effect of that factor on the UFP levels.

- 2023 RSG & KLM: Employee Exposure Research

People from seven different roles each received a measurement set, consisting of a UFP meter and a PM meter, both of which measure concentrations, to carry on their body. For three days, during every shift with a minimum duration of 6 hours, 2 employees per role performed their normal job with these sensors. The roles included: platform employees (KLM) on Pier D (Airbus 320 & B737 planes) & pier E (B777 & B787 planes), platform employees (Menzies) on pier C (Cargo planes), platform employees (Dnata) Pier C and Pier G (multiple plane types), service employees (Axxicom), marshallers (RSG) and employees working inside the baggage hall (KLM). Next to this, continuous measurements of 8-hour timeframes during the employee shifts in a period of 3 weeks on set locations at the D & E pier. Also, background measurements of UFP and PM took place during 3 days to gain insights in the emission caused by frequent occurring situations

- 2023 Amsterdam Airport Schiphol continuous measurement research lab

In July 2023, at Amsterdam Airport Schiphol 10 UFP sensors were installed on two different aprons (Figure 1) to continuously measure ultrafine particle (UFP) concentrations and analyze the behavior of these particles under various circumstances. The selected location, surrounded by buildings and runways, is based on a TNO study conducted in 2021, which identified D23 and D44 as areas with potentially the highest UFP concentrations of the airport. These 10 sensors, more specifically the Naneos Partector, can measure particle sizes down to 10nm continuously per second. The collected data is integrated with flight and weather data to provide a comprehensive understanding of UFP dynamics. In this learning environment, UFP measurements are conducted for research purposes, validating the effectiveness of innovative measures and accelerating improvements in air quality. However, to generate valuable insights, the sensors need to collect data for at least one year to compare different influences and scenarios. As such, the results of these ongoing measurements are not included in this report.

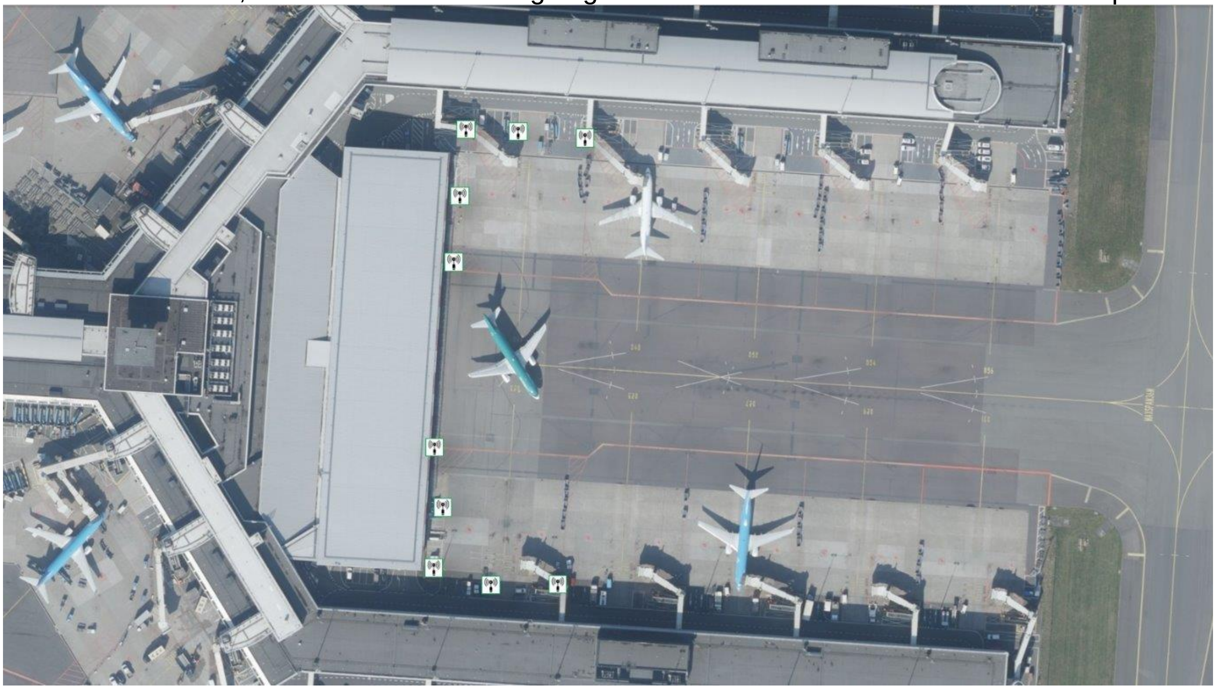

Figure 1 Placement of UFP sensors at the apron

3.3 Overview UFP measurements and experiments with used sensors and measurement data points

Measurements and experiments	Used sensors	Measured datapoints
• 2022 Amsterdam Airport Schiphol: Droplet Screen Experiment • 2022 TNO Eindhoven Airport: UFP Concentrations • TNO Rotterdam Airport: UFP Concentrations • 2022 Amsterdam Airport Schiphol: Overpressure Experiment • 2023 RSG & KLM: Employee Exposure Research	TSI: • EPC models • SMPS models • CPC Models • UFP Models • P-Trak Grimm: • EDM 465 UFPC Naneos: • Naneos Partector Oxility: • Aerasense Nanotracer Dekati: • ELPI+	• UFP concentration • GPS location • Black carbon concentration • Wind speed • CO_2 concentration (vol%)

3.4 Key insights of what we know through the measurements and experiments performed

UFP Concentrations

UFP from aircraft turbines tend to be smaller in size (10-16 nm) and higher in concentration than UFP from other combustion engines (10-300 nm). The highest UFP concentrations from aircraft turbines are found close to the runways, piers and terminals with peak concentrations around 200,000-300,000 #/cm^3 found during measurements in 2015. These concentrations most likely represent the maximum range of the sensors during that time. These UFP concentration peaks at Amsterdam Airport Schiphol were related to 'jet blast events' of airplanes starting their engines, taxiing and taking off. As such the UFP concentrations measured in 2021 vary greatly over time and location from 10,000 to 300,000 #/cm^3 with the highest concentrations during the morning timeslots. During the measurements at Rotterdam in 2022, peak concentrations up to the maximum of the sensor range 1M #/cm^3 were found. A factor that significantly influences UFP concentrations at different locations is the wind. High wind speeds and wind directions coming from the platform and runway cause significantly higher levels of UFP concentrations than low wind speeds and opposite wind directions.

Employee exposure to UFP Concentrations

Airplane movements and running APU's cause UFP peaks in exposure concentration for outside platform employees, while exposure levels for people working inside the baggage hall stay relatively low. As such, exposure to UFP levels is highest for employees who work outside on the platform for a long period of time, and close to airplane movements. There are no insights yet on consequences of UFP exposure for employees, but a research with a test group in a lab and inhabitants around Amsterdam Airport Schiphol showed that short term exposure to UFP levels can temporarily increase existing respiratory conditions. The effects on heart and vascular system, birth outcomes, the nerve system, metabolism and general health were measured as well, but a relationship with UFP was only indicative or not found.

Sensors

Throughout the different measurements performed at Amsterdam Airport Schiphol, 11 different types of sensors were used to measure UFP levels. The technology of these sensors is in continuous development, and at least 4 out of 11 are already out of date and are replaced by newer versions which explains the high amount of different sensors used. The sensors were produced by TSI, Grimm, Oxility, Dekati or Naneos and owned by RSG, TNO, Vito or ECN. The most commonly used sensor for RSG measurements is the EPC sensor from TSI (model 3781). This sensor was used by TNO for UFP concentration measurements at Amsterdam Airport Schiphol, Rotterdam-The Hague Airport and Eindhoven Airport. This sensor is deemed reliable for counting the number of particles in the measurement range, including UFP from aircrafts, alternative sensors for the

EPC sensor, tested at Rotterdam Airport did not live up to the expectations and provided results with too much inaccuracy.

Continuous measurements and Mitigation Methods

To reduce UFP concentrations at RSG based on our previous learnings, several future studies are proposed. However, these measures have not yet been assessed in an continuous operational setting, and UFP sources and levels have not been investigated in real-time operations. Continuous measurements help in understanding the behaviour of UFP. To gain a better understanding of UFP levels and sources within airport operations for RSG's own learnings and WP7.1, the Research Lab is established. This Research Lab, located airside at Amsterdam Airport Schiphol, will measure current UFP levels and facilitate testing to determine the impact of various measures and external influences that we believe will affect UFP levels based on previous experiments and measurements.

In addition to this Research Lab, our learnings have identified two innovative mitigation methods that are worth exploring in experimental setups. One involves what this report entails, using water to cluster UFP, causing it to fall to the ground before it can be inhaled. Initial results, of the test of 2022, indicate a downward trend in UFP concentrations, though the reduction is not yet significant. Further optimization of this strategy is warranted. Another approach is creating overpressure inside buildings and filter the air with a HEPA filter to keep UFP concentrations low. Initial tests show that this method effectively maintains low indoor UFP levels by using filtered air to create overpressure. Both experimental measures will continue under various conditions to validate their potential effectiveness.

4 Literature evaluation of effectiveness of water droplets in UFP mitigation

This section summarises the findings from literature on how water can be used to lower the concentrations of UFP in exhaust emissions and how these findings have been converted into design requirements for a water dispersal system, aimed at lowering UFP concentrations from the jet exhaust at engine start-up.

4.1 Good practices, no guidelines

UFP is defined as particulate matter with a diameter equal or less than 0.1 micrometre (µm). The main sources of UFP are internal combustion engines used in transportation, industry, power plants and residential heating. Exposure to UFP can increase the likelihood of certain types of heart diseases. Due to the small particle size, UFP can penetrate deeper into the lungs, resides there for longer periods of time and can reach other organs via the bloodstream. This makes it likely that UFP is more harmful than other types of PM. (RIVM, 2023; WHO, 2024).

According to WHO, research is still inconclusive on the long-term health effects of exposure to UFP and as such there is insufficient data to provide air quality guidelines. According to their global air quality guidelines, WHO finds enough evidence to recommend the following good practices for UFP:

1. Quantify ambient UFP in terms of particle number concentration (PNC) with a lower limit of ≤ 10 nanometer (nm) / 0.01 µm and no restriction on the upper limit
2. Include UFP monitoring into existing air quality monitoring. Include size segregated measurements at selected stations continuous and in parallel with other airborne pollutants
3. Distinguish between high (24h mean: > 10,000 #/cm^3; 1h mean: 20,000 #/cm^3) and low (24h mean: < 1,000 #/cm^3) PNC
4. Utilize emerging science and technology to update UFP approach

(WHO, 2021)

4.2 UFP and aviation

4.2.1 UFP emissions from aircraft

Section 4.2.1. is copied with permission from Simon Christie of Manchester Metropolitan University

In general, the UFP aerosol life cycle includes emission, gas-to-particle partitioning, transport, physical and chemical processing, particle-to-gas partitioning, and deposition of particles. Within these broad categories, aircraft emissions are known to undergo a number of aerosol microphysical processes, including:

- gas–particle partitioning of semi-volatile species;

- condensation of non-volatile H_2SO_4;
- formation of secondary organic particles;
- new particle formation by nucleation;
- particle coagulation.

However, the parameterisation of aerosol formation at downwind distances is poorly understood. Most models predict a rapid rise in concentrations as the plume cools followed by a progressive reduction in concentration due to dilution, dispersion and losses[2].

Earlier studies represented the size distribution of the engine plume at cruise altitude with one particle number size mode at 25 nm and a larger mode at 150 nm (Petzold et al., 1999). More recent studies based on ground measurements in engine exhaust plumes (20 m behind engine exit) found particle size modes at 10 nm and a larger mode at 35 – 40 nm (Schripp et al., 2018). Brilke et al. (2020), who conducted measurements approximately 500 m downwind of a runway, reported on a particle size mode at 10 nm (nucleation mode) and two larger modes at 50 nm (Aitken mode) and 150 nm (accumulation mode), respectively. These findings are consistent with several previous studies which measured aircraft engine PM emissions downwind of active runways (e.g. Mazaheri et al., 2009; Lobo et al., 2012; Chan et al., 2016).

The systematic measurement of non-volatile PM (nvPM), total PM (TPM) and speciation of the volatile PM (vPM) at downstream distances are not reported in the literature. This is one of the deliverables from the AVIATOR project, but it is yet to be published. A typical size distribution for two different fuels at a downstream distance of 50 m and 7% thrust is shown in Figure 2.

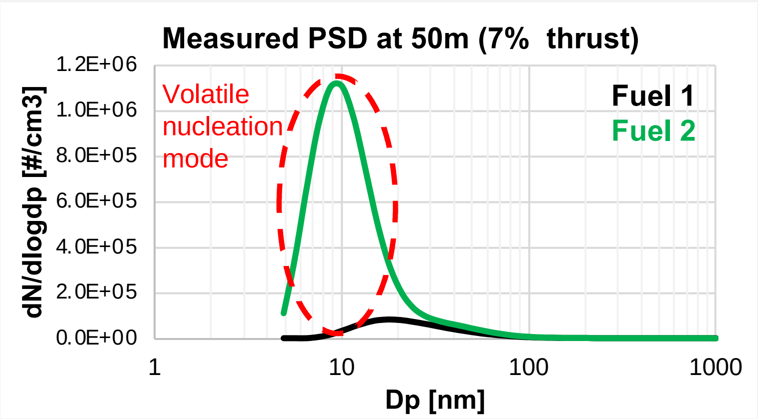

Figure 2: measured PSD at 50m (7% thrust)

Key results:

- There is a prominent UFP nucleation mode of volatile particles downstream of engine exit.
- Sulphur in the fuel can have a significant effect on the size distribution and number of UFP.

[2] According to the authors this stresses the importance of a measurement of UFP (size dependent) and parameters like windspeed/direction, temperature and humidity during UFP measurements.

- The greater prominence of the volatile peak measured at low thrust is related to temperature and transport time.
- Number concentrations for vPM >> nvPM within relatively short distances.

Typically, results for the ratio of total PM to nvPM are shown in Figure 3.

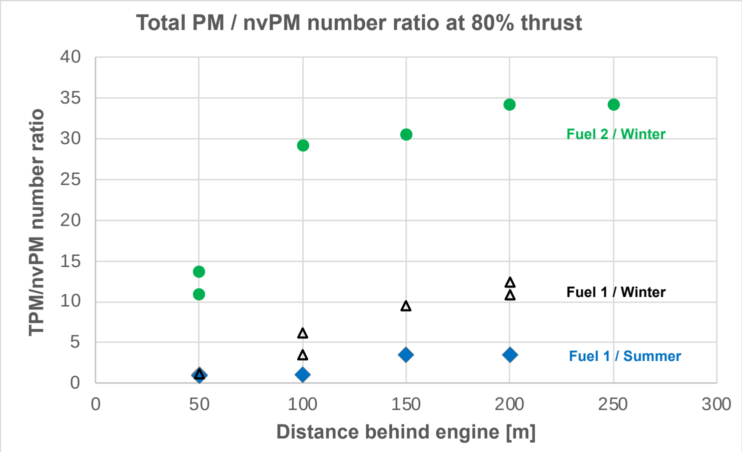

Figure 3: TPM/nvPM ratio at increasing distances behind engine (80% thrust)

Key results:

- TPM/nvPM ratio increases with distance (indicating PM formation)
- TPM/nvPM ratio are higher for higher sulphur fuels (fuel 2).
- For the same fuel, the TPM/nvPM ratio is higher in winter (i.e. there is probably a dependence upon ambient conditions such as temperature and humidity)

In addition, modelling studies have shown that the presence of stabilising species within the ambient air (such as ammonia and amines) can impact total PM formation rates and stability.

Volatile PM strongly depends on both time and temperature, apart from the emissions and its dispersion, while non-volatile PM can be considered roughly constant on short time scales in which the emission sources and wind field do not change significantly. In addition, the use of a spray system may introduce aqueous UFP that additionally also strongly depends on time and temperature. For the *spray off* situation, this could be summarized as follows:

$$\mathrm{UFP}_{\mathrm{spray\ off}} = \mathrm{nvPN}(\bar{T}, w) + \mathrm{vPM}(\bar{T}, w, t, T)$$

Here, $\bar{T}$ indicates engine thrust setting, w indicates wind field, t indicates time, and T indicates temperature. For the *spray on* situation, however, the following would apply:

$$\mathrm{UFP}_{\mathrm{spray\ on}} = [\mathrm{nvPN}(\bar{T}, w) + \mathrm{vPM}(\bar{T}, w, t, T) + \mathrm{aqueous\ UFP}(\bar{T}, w, t, T)] \times (1 - \mathrm{removal\ efficiency})$$

Downstream Dilution Factors

The shear between the ambient air and thrust from the aircraft engine (core and bypass) creates a highly turbulent environment that rapidly entrains air, expands and cools. Dilution factors are dependent upon the downstream distance and engine thrust setting. Estimates of the expected dilution factor for the specific airframe/engine combination can be made from the profiles in the aircraft manual.

In an experimental setup, dilution factors are often determined with reference to a measured carbon dioxide (CO_2) concentration. However, as the dilution increase to >100, the difference between engine CO_2 and ambient CO_2 is increasingly difficult to determine and the uncertainty rises. In this case, cross check methods may be judicious.

4.2.2 Health impact of UFP from aircraft

Aircraft emit UFP and people who live close to a larger airport are regularly exposed to higher concentrations. The impact of UFP emissions from aircraft engines on local air quality and health is generally less understood than the impact of other emissions such as PM_{10} and nitrous oxide (NO_x).

Two recent studies stand out:

A 2020 study of incidences ischemic heart disease[3] and cerebrovascular disease[4] among airport workers at Copenhagen Airport showed no increased incidences compared to a control group, in fact risk levels were higher in the control group. The number of years working on the platform did not corelate to the outcomes. (Møller, et al., 2020)

A 2022 study of the short and long term health effects of exposure to UFP emissions from aircraft among residents living near Amsterdam Airport Schiphol. showed that short term exposure to UFP can aggravate existing respiratory diseases especially among children. There are no indications that long-term exposure to aircraft UFP can cause respiratory diseases. Long-term exposure "may possibly have an effect on the cardiovascular system" and "may possibly have a detrimental effect on the development of unborn children". The researches speak of a 'possible effect' as there is too much uncertainty to conclude that there is causal relation. There is also "insufficient scientific evidence to suggest that exposure to aircraft UFP has an impact on the nervous system or causes diabetes". 'Insufficient evidence' means that the results of the sub-studies of this study are either contradictory or unclear and that an insufficient number of other studies has been carried out. With the exception of a possible effect on death from arrhythmia[5], there are no indications that people die sooner if they are exposed to ultrafine particles from air traffic over many years. (Janssen, Houthuijs, & Dusseldorp, 2022)

[3] Most common type of cardiovascular disease, involves clogged arteries of the heart
[4] Involves clogging of the blood vessels of the brain and cerebral circulation
[5] Irregular heart beat

Key results: Both studies fail to conclude on a causal relation between exposure to UFP from aircraft and health effects. However, this does not mean there is conclusive evidence to dismiss concerns about aircraft UFP emissions and health. More research is needed to conclude on the health impact of UFP emissions from aircraft and a cautionary approach is advised.

4.3 Using water for UFP mitigation

Whilst water is commonly used to suppress dust from building activities or mining, using water to lower concentrations of much smaller UFP in transportation is still very experimental.

One recent example is a study by the Polish Academy of Sciences that investigated emission reduction of particulate matter from marine diesel engines using electrically charged water particles (Sobczyk, Jaworek, Marchewicz, Krupa, & Czech, 2019).

Key result: Whilst the results are promising, high voltage charging particles in airport environment raised safety concerns that were deemed insurmountable within the project and was thus dismissed.

One study from 1984 by the University of Arizona investigated the use of charged water droplets of various diameters and using different means of charging to control fugitive dust from emissions. One of the means of charging the particles that was discussed was the autogenous charging of de-ionized water by means of grounding the spraying nozzle and thus removing the need of high voltages (Mathai, 1984).

Key results:

- Overall, the study showed fine, charged particles to be an effective means of controlling fugitive dust from emissions. Charging increased the efficiency with 78% compared to the non-charged droplets.
- Relative humidity plays a significant role in determining the overall particle collection efficiency. The lifetime of the droplet is the dominant factor in determining the particle control efficiency. A lower relative humidity and/or higher temperature of the environment, shortens the lifetime of the droplets, and therefore the effective reduction volume.
- For larger particles, aerodynamic diameters greater than 2 - 3 µm, the dominant mechanisms of particle collection are impaction and interception. For particles smaller than 0.1 µm (< 100 nm), Brownian motion becomes more important, for particles of 100 nm to 2 µm, electrostatic forces become important.

Of course there is also a natural source of water droplets: rain. A Finnish study determined the rate at which rain droplets can coagulate UFP (called scavenging) by measuring UFP concentrations during rainfall. The results were used to develop an improved prediction model for the amount of scavenging by rain (Andronache, Grönholm, Laakso, Phillips, & Venäläinen, 2006).

Key results:

- Scavenging coefficients with "median values in the range of 7 x 10^{-6} to 4 x 10^{-5} per second" were observed at a boreal site in Southern Finland over a period of 6 years
- Observed scavenging rates matched previous observations but proved higher than expected from existing models
- Results showed that the amount of scavenging was dependent on the size of the UFP particles, rainfall intensity and atmospheric effects inside cloud elements. Smaller UFP particles (32 nm diameter) were more sensitive to rainfall intensity than larger particles (340 nm diameter)

The improved model was "significantly sensitive to the choice of representation related to mixing process, raindrop size distribution, phoretic effects in aerosol-raindrop collisions and cloud droplet activation"

4.3.1 Measuring UFP concentrations

To accurately measure the UFP concentrations behind the Cessna Citation 550 and assess the potential effect of the water spray system, several key considerations must be taken into account when designing the experiment, such as environmental conditions, particle behaviour and the influence of the equipment that is used for the experiment.

UFP are characterized by their small size of 100 nm or less, which is a challenge for conventional mass-based air quality measurements. A common method to quantify UFP is a count-based approach. (TSI, n.d.) Every particle (with a diameter below 100 nm) is counted and represented as a number of particles in a given air volume, e.g. #/cm^3. This information can be used to assess particle formation, transport and human exposure. More information can be retrieved if the measurement equipment has a sizing capability, besides the counting capability. This allows for a representation of the particle size distribution of the UFP which makes it easier to find a specific source and changes in the distribution of sizes.

The appropriate sampling method requires the consideration that the sample aerosol may be in a condensing or evaporating environment, which could change the size and total mass of aerosol material. (Kulkarni, 2011) Conditioning the sample through heating may be necessary to ensure representativeness.

The spatial and temporal variation of UFP particle concentrations are high due to external influences such as traffic, season (such as temperature and relative humidity) and weather conditions (such as wind and precipitation). (Viitanen, 2017) These factors must therefore be kept as constant as possible to allow for a correct comparison of measurements taken at different times.

The theoretical diffusion losses in a tube were analysed by calculating the fraction passing through the tube. The equations are from Aerosol Measurement, edited by Baron and Willeke (2001). The penetration fraction of UFP reaching the sensor in the transportation using a tube is estimated and shown in Figure 4 for a turbulent flow. This equation does not account for different concentration levels, or possible saturated tube walls. The losses show that the measured UFP could be significantly lower than the actual UFP concentration in the plume, as typical diameter particles from the plume are around 10 nm.

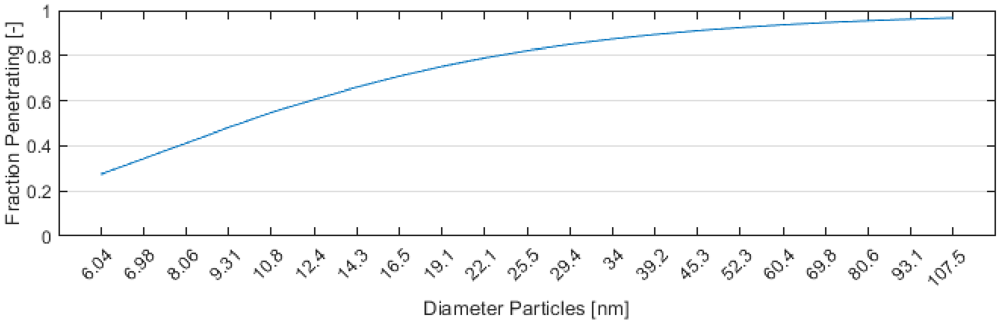

Figure 4: Estimation of the penetrating fraction reaching the sensor for the bins up to 107.5 nm, assuming turbulent flow. (Baron, 2001)

5 Methodology

5.1 Design of the water delivery system

Mitigating UFP or PM concentrations with water is not a common practice. As such, no commercial off-the-shelve solutions were found that could deliver large amounts of the droplets specified in the section above. Spraying Systems Co., a company headquartered in Illinois USA specialised in the design and manufacturing of spraying nozzles, was approached to design and build a water delivery system for the experiment.

Spraying Systems Co. was asked to:

1. Determine the optimal nozzles for the water system
2. Determine the required number of nozzles for a prototype water delivery system to be used in the main experiment
3. Determine the required pressures and flow rates

After measuring the water droplet size for different nozzle types, Spraying Systems Co. identified the SU16-SS as the best suited nozzle as it was able to deliver small enough water droplets (measured in D32) at modest system pressure (<5 bar). Using their proprietary VOA (Virtual Overlapping Analysis) software Spraying Systems Co. was able to design the water delivery system which consists of 4 identical frames that are mounted vertically, 1.5m off the ground. Each frame caries 56 nozzles distributed across 8 horizontal lines. Connected to the water delivery system are a water pump and an air compressor. The water delivery system is shown in Figure 5.

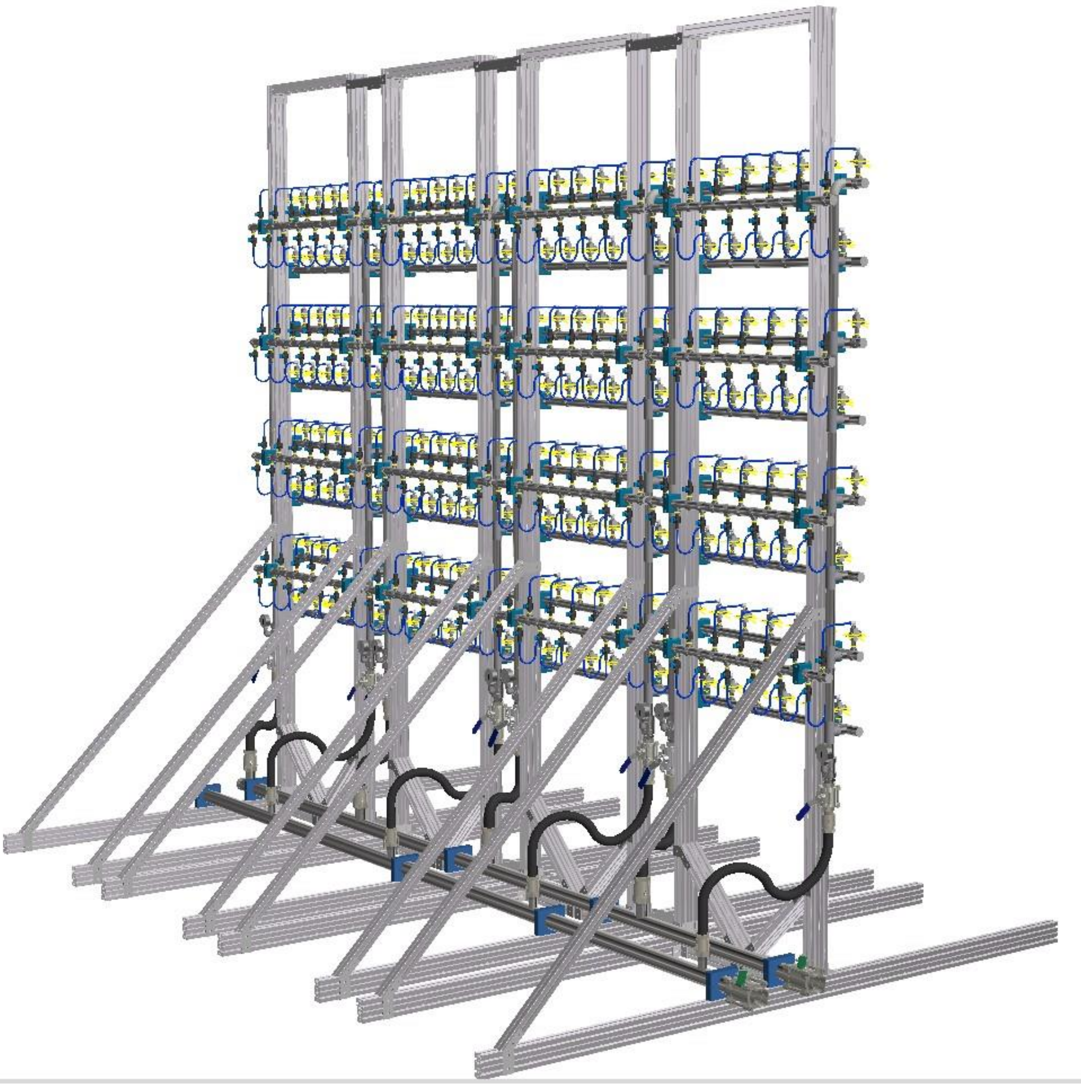

Figure 5: design drawing of water spray system (©Spray.com)

Main specifications:

- Nozzle type: SU16-SS
  - Produced water droplet diameter: ca. 8 µm (D10, arithmetic mean)
  - Water flow rate per nozzle: ca. 0.1 litres/minute
  - Required air supply pressure: ca. 5 bar
- Surface area: 4000 mm x 2000 mm, 1.5 m from the ground
- Number of nozzles: 224 divided over four modular arrays, which can be switched off separately
- Water flow rate of 0.08 liters per minute (lpm) per nozzle (17.92 lpm when full system is operative)
- Air flow rate of ~50 normal liters per minute (Nlpm) per nozzle (11,200 Nlpm when full system is operative)
- Liquid pressure of 60 psi (4.14 bar)
- Air pressure of 70 psi (4.83 bar)

5.2 Experiment design

The main goal of the test campaign was to gather sufficient data in order to determine the (potential) effectiveness of using water droplets (mist) in an airport environment to capture UFP from an aircraft engine during start-up. It should be noted that, due to the novelty of using the reduction technique in an airport environment, the research was of exploratory nature. The study had limited literature and previous experiences to build upon and therefore lacks specific information, for the generic formulation of the best set-up parameters. However, after conducting small scale tests before going to the main experiment with aircraft and water spray system (hereinafter referred to as the ‘main experiment’), some of these parameters were set for further refinement of the measurement goals and objectives in an intermediate stage of the project.

Two small scale tests (pre-tests) were performed before the main experiment. Pre-test 1 and pre-test 2 were designed to determine safe distances for humans and sensors between engine and water spray system, and to familiarize with the equipment that was used during the main experiment.

A concise overview of the set-up parameters searched for in the individual experiments is the following:

1. Pre-test 1 with aircraft: Determine a viable distance aft of the jet engine where the water spray system can be placed during the main experiment.
2. Pre-test 2 with water spray system: Determine a viable distance aft of the water spray system where the sensors can be placed during the main experiment.
3. Main experiment: Quantify the UFP reduction potential of a water spray system and assess the conditions (meteorological, geographical, technical) under which this mitigation strategy can be effective.

In the following paragraphs, concrete objectives and desired outcomes are specified for the individual experiments. Each of the three experiments is performed using a different set of measuring equipment, the full list of measurement equipment is shown in Table 1, which will be referred to in the upcoming paragraphs.

Table 1: List of measurement equipment, with some of its specifications and their usage per test indicated.

Measurement	Specification	Range	Operating Conditions	Pre-test 1	Pre-test 2	Main Test
UFP particle number concentration and size distribution	TSI Fast Mobility Particle Sizer (FMPS) Spectrometer model 3091	Size: 5.6 - 560nm Number: $1{\cdot}10^3$ – $2{\cdot}10^8$	0 - 40°Celsius (C) 0 - 90% relative humidity (RH)		X	X (with dilutor)

UFP particle number concentration	Naneos Partector 2	Size: 10 - 300 nm Number: 0 – $1{\cdot}10^6$	0 - 40°C 10 - 90% RH	x	x	x
Wind Speed and Direction	WindMaster Pro	0 - 65 m/s	-40 - 70°C 5 - 100% RH	x	x	x
Temperature	OIC-406 Temperature & Humidity Node	-50 - 100°C	0 - 100% RH	x	x	x
Relative Humidity	OIC-406 Temperature & Humidity Node	0 - 100%	-50 - 100°C	x	x	x
CO_2 concentration	SEN-STC31	0 - 100 vol%	-20 - 85°C 0 - 100% RH			x
PM, VOC, NO_x concentrations	SEN55	0 - 1000 µg/m^3 (PM), 0 - 1000 ppm (VOC, NO_x)	-10 - 50°C 0 - 90% RH			x
Formaldehyde concentration	SFA30	0 - 1000 ppb	0 - 40°C 10 - 90% RH			x

5.3 Pre-test 1 with aircraft

The aim for pre-test 1 is to measure the plume characteristics of the jet engine that was used in the main experiment; the P&W JT15D-4B mounted on a Cessna Citation 550. This should take away some plume uncertainties concerning the development of temperature, wind speed and relative humidity as a function of distance from the engine exhaust, as well as the expected number of UFP emitted by the engine. Therefore, the aim is to conduct this test with the same engine as the one used during the main experiment, and preferably under comparable meteorological conditions. For the main experiment, a trade-off should be made between coverage of the plume by the screen and appropriate conditions for the measurement equipment. The smaller part of the cone-shaped plume (nearer to the engine) is easier to cover with the screen, while the temperatures nearer to the engine are higher, causing the droplets to evaporate faster, leaving the droplets with less mixing time.

The goals of this pre-test were:

- to determine the conditions behind the jet engine for the purpose of choosing a suitable position for water spray system during the main experiment by:
    - measuring wind speed and wind angle in the center of the plume as a function of distance from the engine;
    - measuring temperature and relative humidity in the center of the plume as a function of distance from the engine; and
- to test the functioning of the Naneos sensor when placed within the exhaust plume, specifically for each distance:

- whether the relative humidity and the temperature of the sampled air inside the naneos is within the operating conditions of the naneos;
- determine the time it takes to stabilize the water spray system at lower UFP levels when the engine is switched off; and
- determine the order of magnitude of the UFP levels behind the engine at a thrust setting of 40%, the breakaway thrust setting for the Cessna Citation 550.

During the test, UFP concentration and meteorological measurements were conducted at 40, 30 and 20 meters from the engine, with an engine running at 40% thrust setting. The test matrix in Table 2 also shows that the measurements were recorded for a duration of 5 minutes at each distance.

Table 2: Test matrix of pre-test 1.

Run	Thrust setting	Distance	Duration
1	40%	40 m	5 min.
2	40%	30 m	5 min.
3	40%	20 m	5 min.
4	0%	20 m	5 min.

Pre-test 1 took place at Rotterdam The Hague Airport (EHRD) on platform A3. The nose of the aircraft was pointed into the wind so that the measurements in the plume would take place downwind of the emitting source while the plume was directed towards the location of the sensors. A schematic top-view of the test setup is shown in Figure 6: Schematic view of the test setup of pre-test 1.. At each distance, the UFP concentration, wind speed, temperature and relative humidity were measured, simultaneously, the wind speed was measured in front of the aircraft for determining the ambient wind conditions. Only one engine (left) was running.

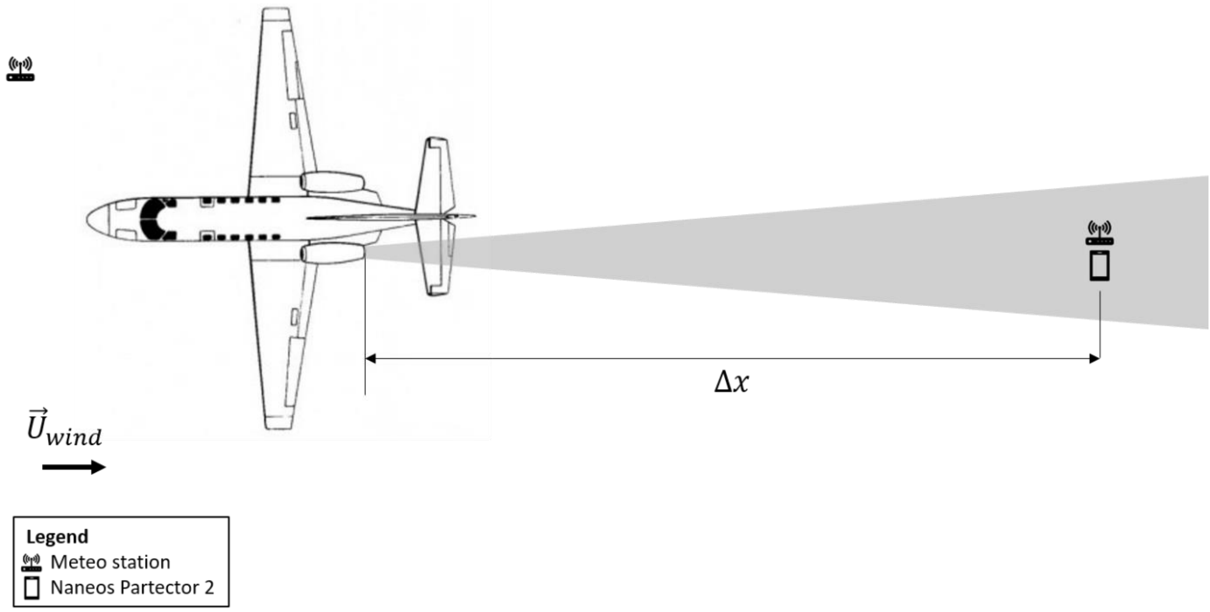

Figure 6: Schematic view of the test setup of pre-test 1.

Following each run, it was determined whether the temperature and humidity levels at the previous distance allowed for a smaller distance towards the engine. A temperature below 40°C and the relative humidity below 90% was required to stay within the sensor limitations as shown in Table 1. Furthermore, the wind speed was not allowed to exceed levels where equipment could fall over. The background traffic during the test was monitored using cameras of which a frame is shown in Figure 7:. The taxiing traffic that was observed passed by downwind of the test section.

Figure 7: Picture of the full pre-test 1 setup during a run at EHRD.

5.4 Pre-test 2 with water spray system

A verification of the UFP measurement approach was done by performing pre-test 2. This involved a check of the correct functioning of all devices in combination with an operating water spray system. The main risk in the setup with the water spray system was that the water droplets could affect the operation of the equipment.

The goals of this pre-test were:

- to determine the conditions downstream of the water spray system for the purpose of finding a suitable distance between the engine and the sensors of the water spray system during the main experiment by:
    - measuring the external relative humidity as a function of distance from the water spray system ; and
    - measuring the external temperature as a function of distance from the water spray system.
- to test the functionality of the Naneos and the FMPS sensor when placed downstream of the water spray system, and specifically for each distance:
    - whether the relative humidity downstream of the water spray system is within operating conditions of both sensors;

- whether the relative humidity of the sampled air inside the sensors is within operating conditions; and
- whether the droplets could have an effect on the UFP and therefore could reduce the measured UFP concentration.

During this pre-test, the UFP measurements and meteorological measurements were conducted from 15 meters to 3 meters distance from the hardware of the water spray system, as shown in the test matrix in Table 3.

Table 3: Test matrix of pre-test 2.

Run	Distance	Duration
1	15 m	2 min.
2	13 m	2 min.
3	11 m	2 min.
4	8 m	2 min.
5	5 m	2 min.
6	3 m	2 min.

Pre-test 2 was conducted at Twente Airport (EHTW) at an engine test site. The minimum distance for the sensors to the engine, while staying within their operational limitations, was used from the results of pre-test 1. This distance corresponds to a measured flow speed of 8.7 m/s in the plume on average, at 20 meter distance at comparable meteorological conditions. At each distance, the UFP concentration (measured by the Naneos), wind speed, internal and external relative humidity and temperature were measured downstream of the water spray system, together with the ambient wind speed upstream of the water spray system. An electric fan was prepared to simulate the acceleration of the flow by the aircraft engine, however, the ambient wind on the test day dominated the flow speed of the fan. Therefore, the fan was redundant and withdrawn from the tests. The ambient wind could not be set, however, the wind speed and direction were relatively constant throughout the measurements. The heat effect of the engine exhaust, affecting relative humidity and temperature in the flow, was not simulated during this experiment. A schematic view of the final test setup is shown in Figure 8:. The FMPS was used to measure UFP concentrations downstream of the water spray system after having the confirmation that the humidity was below 90% at a certain distance, this measurement was used to analyze any effect that the water spray system (with air and water) could have on the UFP measurements.

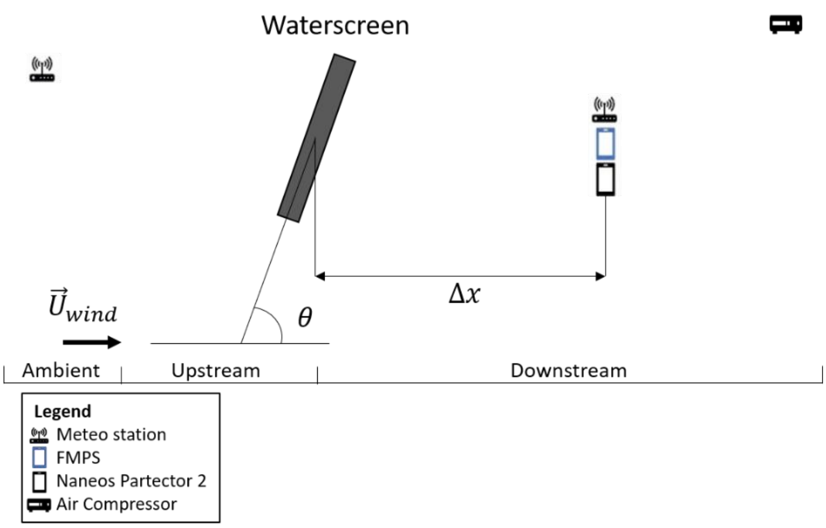

Figure 8: Schematic view of the test setup of pre-test 2.

After each run, it was observed whether the humidity levels at the previous distance allowed for decreasing the distance to the water spray system. The relative humidity was required to stay below 90% for the sensors to operate correctly. There was no background traffic during the test.

Figure 9: shows a picture of the water spray system during a run, where the water droplets are carried by the ambient wind, downstream of the test section. Contaminated air might be drawn by the air compressor and introduced into the test section through the water spray system. The pre-test included measurements to check the significance of the contamination by the air compressor.

Figure 9: Picture of the water spray system operating with the flow directed into the ambient wind during pre-test 2 at EHTW.

5.5 Main experiment with aircraft and water system

The goal of the main experiment was to quantify the UFP reduction effectiveness of the water spray system (with de-mineralised ionised water) in the plume of a jet engine at breakaway thrust setting. The same engine type was used as in pre-test 1, the P&W JT15D-4B on a Cessna Citation 550. Both pre-test 1 and pre-test 2 helped to determine adequate distances between the sensors, the engine and the water spray system, to operate safely and accurately.

The goals of the main experiment were:

- to quantify the UFP reduction potential of a water spray system by:
    - measuring the total UFP concentration (#/ cm^3) at three locations using the Naneos;
    - measuring the UFP concentration (#/ cm^3) per diameter bin at one location using the FMPS in combination with a dilutor that dilutes the concentration by a factor 100, to prevent oversampling the sensor;
    - measuring the speed and angle of the plume and the ambient wind or flow at two locations;
    - measuring the relative humidity and the temperature in the plume at one location using the OIC-406 sensor; and
    - varying thrust setting and water spray system setting (on/off) by observation.
- to assess the conditions (meteorological, geographical, technical) under which this mitigation strategy can be effective.
- to provide recommendations for using the water system in an airport operational environment by:
    - validating whether a water spray system can significantly reduce UFP concentrations in the exhaust plume of an aircraft;

- validating the UFP measurement setup and optimize the experimental setup parameters;
- understanding the interplay between various testing parameters and the measured reduction of UFP concentrations; and
- acquiring experience and knowledge about the water spray system to be able to refine the water system design for a future experiment.

Table 4 shows the test matrix of the main experiment. Run 1 and run 2 are identical, where only 40% thrust was tested with every possible setting of the water spray system. During run 3, the 28% thrust setting was added. The water spray system has three possible settings: off, only air or air and water. Every run starts with a background measurement where the engine and water spray system are both off. This is the background measurement at the start of each run. Every test with a unique combination of variables in each run is measured with a duration of 5 minutes. The experiment is focused on showing the potential effectiveness of the water spray system with air and water, compared to the case where the water spray system is off. The tests with only air were used to see how the addition of the water volume affects the UFP concentration and what the effect of only air is. It was used to show whether the introduction of kinetic energy by air just in front of the water spray system, independent from the effect of water, affects the UFP concentration. The difference in dilution of the flow with air, or water and air, can be analysed using the flow rate of the air compressor, however these flow rates were insignificant for the measured results compared to the flow rate of the engine. Every run is finalized with a test where the engine is off and the water spray system on with air (A) and water (W).

Table 4: Test matrix for the main experiment.

Run 1 Test	**Thrust setting**	**Water spray system setting**	**Duration**
1	0%	Off	5 min.
2	40%	Off	5 min.
3	40%	A	5 min.
4	40%	A + W	5 min.
5	0%	A + W	5 min.
Run 2 Test			
1	0%	Off	5 min.
2	40%	Off	5 min.
3	40%	A	5 min.
4	40%	A + W	5 min.
5	0%	A + W	5 min.
Run 3 Test			
1	0%	Off	5 min.
2	28%	Off	5 min.
3	28%	A	5 min.
4	40%	A	5 min.
5	28%	A + W	5 min.
6	40%	A + W	5 min.
7	0%	A + W	5 min.

The main experiment was performed at Twente Airport (EHTW) at an engine test site, where pre-test 2 was performed as well. During the measurements there was no other traffic monitored on the airport.

Figure 10: shows an overview of the test setup. Upstream and downstream directions in this report refer to the flow direction of the engine exhaust. Pre-test 1 and pre-test 2 have shown that the operating conditions, such as the temperature and the relative humidity, were not exceeded at the distances shown in Figure 10:.

Downstream of these sensors, an array of nine low-cost sensors (LCS) was placed with a two meter spacing between each sensor, one LCS-sensor was placed upstream for background measurements. Every LCS-sensor measured the concentration of CO_2, formaldehyde, VOC, NO_x and PM concentration levels. The array of these sensors was used to indicate the location of the jet engine plume downstream of the UFP sensors to ensure the correct location to measure the exhaust concentrations.

The Naneos sensors up- and downstream of the water spray system were used to show a change in the difference of UFP concentrations across the water screen. The three devices are from the same production batch and were calibrated by the factory in the same way.

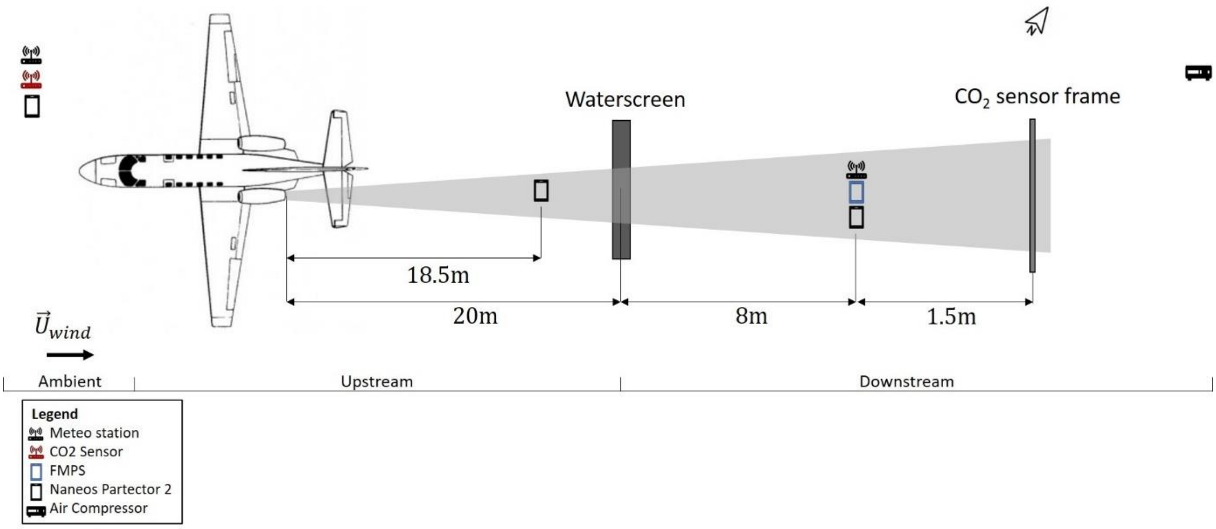

Figure 10: Schematic view of the test setup of the main experiment (actual wind direction was different during the 2nd test, see section 6.3.1).

After each run it was checked whether the concentration levels of all the sensors stabilized to the background levels, before proceeding with the next run. Pictures of the test setup during the measurements are shown in Figure 11: shows the side view, and Figure 12: shows the rear view.

Figure 11: Side-view picture of the test setup behind the aircraft during the measurements for the main experiment.

Note how the amount of water spray appears significantly less as during pre-test 2 (Figure 9) as a result of the exhaust plume from the running engine

Figure 12: A picture from behind the test setup of the main experiment.

As the aerosol measurements by the FMPS could not be made in situ, the sampled air was transported through a silicon tube with a length of 14.2 meters to the FMPS, situated in the car downstream of the water spray system. As discussed in Section **Error! Reference source not found.**, smaller particles show larger losses, however, the actual losses are expected to be lower due to high concentrations and saturated tube walls. The measured particle numbers are underestimated, especially when it is considered that a loss of around 50% is possible for 10 nm particles. The setup and the tubing has not moved or changed during the day of the experiment. Therefore the absolute losses in the tube between the different runs did not change significantly. The external relative humidity was kept under the operating conditions of the sensors, while internal heaters were used to dry the sampling air of the FMPS and the Naneos.

5.6 Analysis plan of the main experiment

Based on previous experience and literature, the measured UFP concentrations are expected to be highly variable in space and time. The main goal of the analysis plan for the main experiment was to identify and quantify this variation due to the workings of the water spray system, using the knowledge as obtained from the pre-tests. The main objective is to assess if a water spray system has the potential to reduce UFP concentrations in an airport environment. To achieve this, three metrics are used:

- UFP particle count, using the bins from 5.6 nm to ca. 100 nm (FMPS).
- The difference in total particle count as measured concentration by the Naneos downwind of the water spray system and the measured concentration by the Naneos upwind of the water spray system.
- The difference in lung-deposited surface area (LDSA) as calculated by the Naneos downwind of the water spray system and the measurement by the Naneos upwind of the water spray system. The LDSA calculation is done by the Naneos based on diffusion charging, approximating LDSA as being directly proportional to the measured charge.

Alongside the effect of the water spray system on the UFP measurements, background concentrations and meteorological conditions also cause part of the measured variability. The measurement setup has been designed as such that an important part of this unwanted variability due to external factors could be corrected for when analysing the test results. This is embodied by the use of:

- multiple identical Naneos Particle II sensors:
  - two installed in the engine plume; one in front and one aft of the water spray system to quantify any changes in particles density across the water spray system. The time-variant external factors are assumed to have influenced both sensors in a similar way;
  - one installed outside the plume, to quantify the (variations in) background particle densities;
- two meteorological stations to measure (changing) wind conditions. Temperature and relative humidity measurements are only used to define the time windows of various measurement conditions by looking at the moments where those quantities roughly stabilise.

Furthermore, the validity of individual measurement has to be verified. This is done through:

- internal temperature and relatively humidity sensors within the FMPS and Naneos devices. These are used to verify if the temperature and relative humidity fall within operational limits of the devices;

- a set of nine LCS clusters to allocate the lateral displacement of the plume around the UFP sensors behind the water spray system; and
- quality flag logs of the meteorological stations.

Any invalid data must be filtered out. All aforementioned steps regarding data selection are part of a broader framework which is adhered to, called the Cross-industry standard process for data mining (CRISP-DM, Chapman, et al. (2000)). More details on this can be found in Appendix A.

After filtering and reformatting all data from the measurement day, the variations over time of wind conditions and background particle density are accounted for by a technique combining Principal Component Analysis (PCA) and clustering (Jolliffe & Cadima, 2016). These techniques aim at comparing particle density measurements from different measurement conditions (e.g. water spray system on or off) under similar wind and particle background conditions, for a fair comparison. The technique is further elaborated on in Appendix B.

6 Results and Discussion

This chapter describes the test results of pre-test 1, pre-test 2 and the main experiment. Throughout the chapter the different conditions will have the same naming convention. The thrust of the engine will be specified by the percentage of the thrust level followed by 'T' of thrust. E.g. 40% thrust is shown as 40T. The water spray system has two possible settings, air on and water and air on. These are displayed as 'A' and 'A+W', respectively. It is assumed that the pressures and flow velocities of the water and air are constant over time.

6.1 Pre-test 1 with aircraft

Figure 13: shows the results of the ambient wind- (speed and direction), temperature and humidity over time at different distances from the engine. The wind speed shows a significant difference, as the flow is accelerated by the jet engine. The mean velocity of the ambient wind is 4.2 m/s, and the mean velocity in the plume ranges from 7.2 m/s to 8.7 m/s, at a distance 40 meters to 20 meters from the engine, respectively. The ambient wind conditions had missing data points, as the Windmaster Pro showed failures during the measurements. The ambient wind- (speed and direction) was experienced as relatively constant, therefore the discontinuous time series are extrapolated and assumed to be representative for the full duration of the test.

Both the external temperature and the external relative humidity in the plume, measured by the meteorological station, showed results that could be expected. The temperature of the flow increased with decreasing distance to the engine and the relative humidity of the flow decreased with decreasing distance to the engine. The ambient temperature and relative humidity affected particle formation and the growth process, however, these were assumed to be constant during the the test.

The temperature and relative humidity of the sampled air was measured inside the Naneos and the FMPS sensors. Both the FMPS and the Naneos have a built-in heater which helped to condition and stabilize the humidity and temperature of the sampling air. The heaters were operational for all the UFP sensors during every measurement. Therefore the temperature of the sampled air inside the Naneos and FMPS varied with less than 2°C during the experiment, which was not significant. These parameters were monitored to ensure that they did not exceed the operational limitations of the sensor and couldn't be used for measuring the outside conditions. The flow velocity, temperature or relative humidity were kept below the set limits at the nearest distance of 20 m from the engine.

All the measurements were performed with an engine thrust setting of 40% and 0% for the background measurement. The engine data was not recorded during the pre-test.

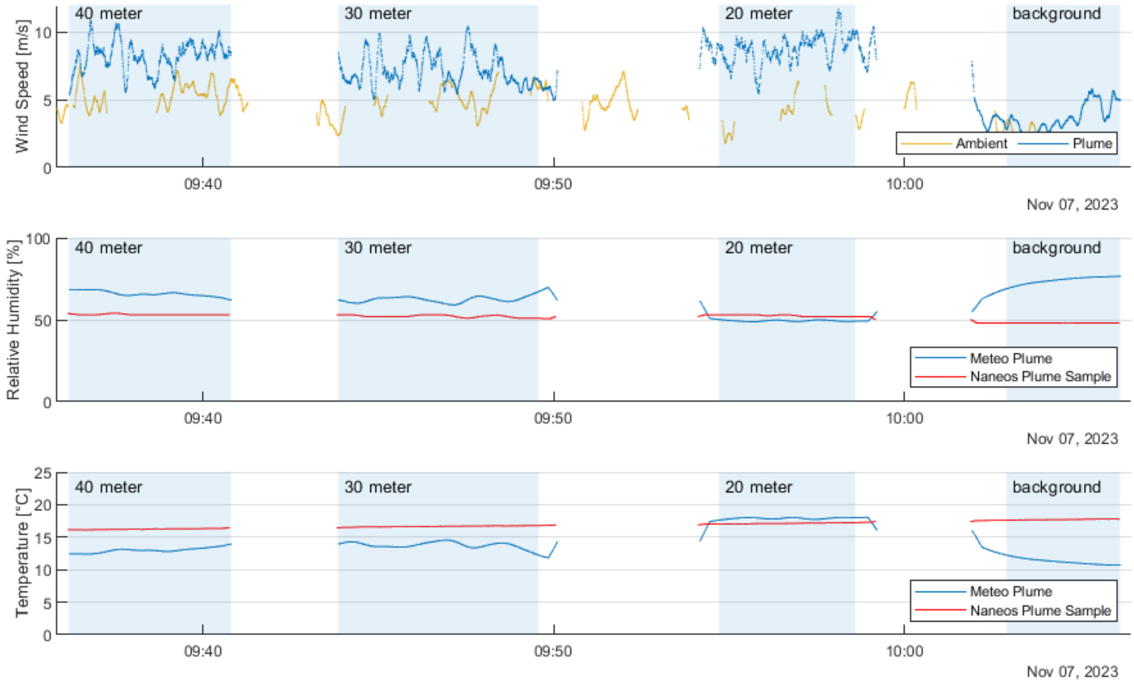

Figure 13: Ambient wind speed in front of the aircraft and flow velocity, relative humidity and the temperature behind the aircraft over time.

The selected measurement data for each distance is indicated in the plot.

The aircraft was positioned with its nose headed into the ambient wind. This results in an engine accelerating the flow into the same direction as the ambient wind. Figure 14: shows a wind rose of the ambient wind and the flow of the plume, which are corresponding well in terms of direction. However, the velocities are generally higher in the plume.

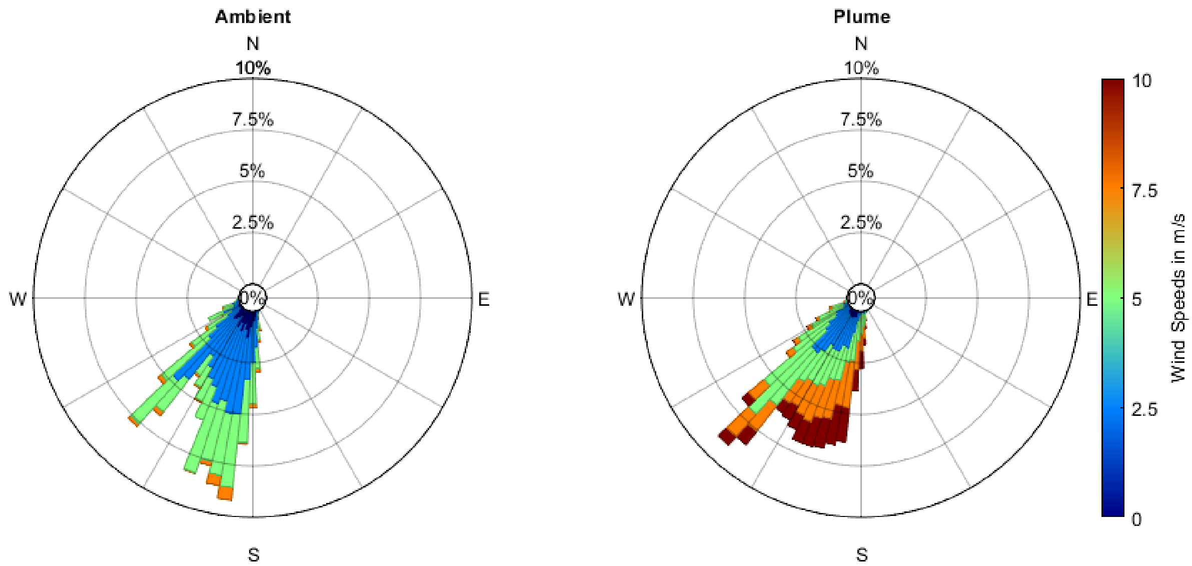

Figure 14: A wind rose of the ambient wind angle on the left, and the plume flow angle on the right showing the aircraft's nose is pointing in the direction of the wind as intended during most of the experiment

The UFP concentrations were measured by the Naneos at each distance from the engine. The concentrations of UFP were expected to increase with decreasing distance from the engine, which is confirmed by the results shown in Figure 15:. The background concentrations were significantly lower than the concentrations measured with engine on. At a distance of 40 meters from the engine, the measured (Naneos) concentrations were in the order of 1.10^7 #/cm^3. At 20 meter, the concentrations were measured in the order of $2{\cdot}10^7$ #/cm^3. The concentrations exceeded the certified limit of the Naneos sensors significantly, which is $1{\cdot}10^6$ #/ cm^3, the error in this range of particle numbers and the effect of the exceedance is unknown. Therefore, much care must be taken when this data is interpreted. Conclusions cannot be drawn using the Naneos measurements solely. The values settled well to background levels when the engine stopped running.

Strong fluctuations of the concentrations were observed, mainly at 40 and 30 meter distance, unfortunately a correlation with the ambient wind could not be found due to lack of ambient wind data in specific time periods. The variety was the lowest at the shortest distance, this might be due to the external factors, such as ambient crosswind or the possible exceedance of the practical measuring limit of the sensor.

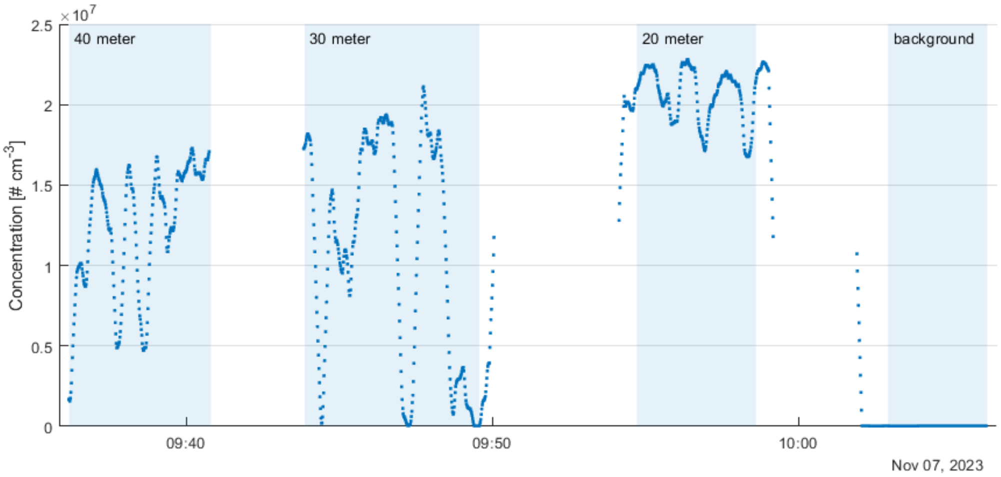

Figure 15: Total UFP concentration (10 – 300 nm) measured by the Naneos Partector 2 in the plume over time. The selected measurement data for each distance is indicated in the plot.

6.2 Pre-test 2 with water spray system

The second preparational experiment, pre-test 2, tested the use of the measurement equipment with the water spray system. The main goals were to determine the appropriate distance between the sensors and the water spray system, without the risk of water damaging the equipment. Efforts were made to simulate the flow speed of the jet engine with a fan (8.7 m/s at 20 m distance), which was determined during pre-test 1 (see Figure 13:). The average ambient wind during this experiment was 4.1 m/s, the fan was not powerful enough to accelerate this flow.

The wind speeds are observed in Figure 16:, the velocities upstream of the water spray system are higher than downstream during the largest period of the measurements. On average, the wind speed was 0.9 m/s lower behind the water spray system. The water spray system introduced air and water with an outflow in the direction opposite to the wind direction, resulting in a deceleration of the flow. The frame of the system contributed to a blockage effect as well.

The relative humidity increases from 83% to 96% on average going from a distance of 11 meters towards 3 meters from the water screen. Similarly to the measurements in pre-test 1, both the internal relative humidity and internal temperature measured by the Naneos showed low variation. The internal conditions of the Naneos were much more stable than the flow temperature and humidity, due to the internal heater.

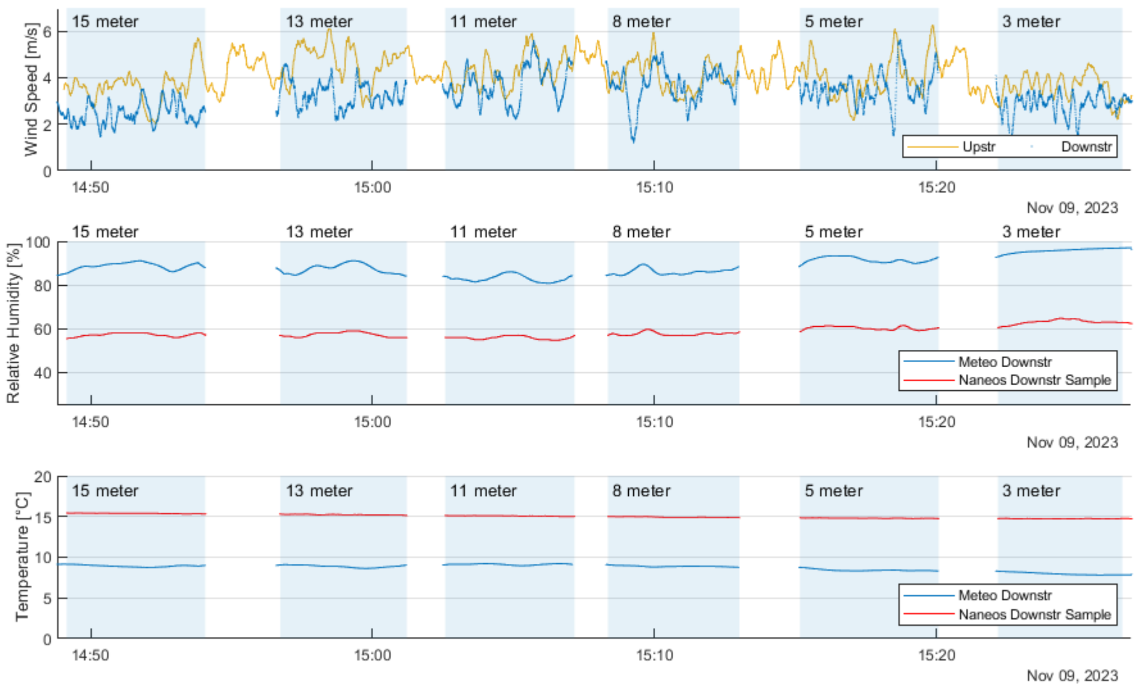

Figure 16: Wind speed, relative humidity and the temperature over time.

The selected measurement data for each condition is indicated in the plot.

The RH inside the FMPS was measured at various distances from the water screen ranging from 3 to 15 meters. 5 meters downstream of the water spray system was identified as the minimum distance for the FMPS in terms of RH. To add some margin for deviating environmental conditions, 8 meters was selected as a safe measurement distance (distance between FMPS and water spray system).

The compressor that was used to pressurize the water spray system had an air inlet near the compressor itself, which is driven by a diesel engine. The effect of the emissions introduced by the compressor were also measured. Affected concentrations could be due to the water droplets, or the 'dirty' air that was introduced by the water spray system. However, the internal heater minimizes the measurement of aquatic particle numbers. The maximum concentrations were derived from this run to establish the worst-case and showed to be insignificant when compared with the concentrations that were measured behind the jet engine during pre-test 1. Figure 17: shows the concentrations (#/cm^3) of each bin size, downstream of the water spray system (A+W).

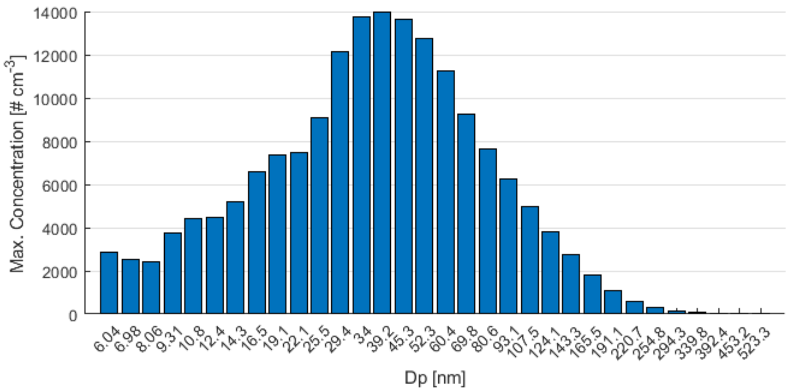

Figure 17: The maximum concentration measured downstream by the FMPS per average diameter bin.

The Naneos was used during all the runs, and the results over time are shown for each distance in Figure 18:. The measurements were performed with a distance to the water spray system of 15 meters down to 3 meters. The UFP concentration measured by the Naneos started increasing significantly at 8 meter distance. The size distribution that was measured by the FMPS at 8 meters, shows a distribution that is to be expected from a combustion source. This suggests that the air outputted by the water screen was polluted by the only nearby combustion source, the exhaust of the air compressor. The internal heaters of the Naneos were used to prevent the measurement of aquatic particle numbers and the internal relative humidity showed stable reading at low levels. Similarly to pre-test 1, the concentrations showed strong fluctuations.

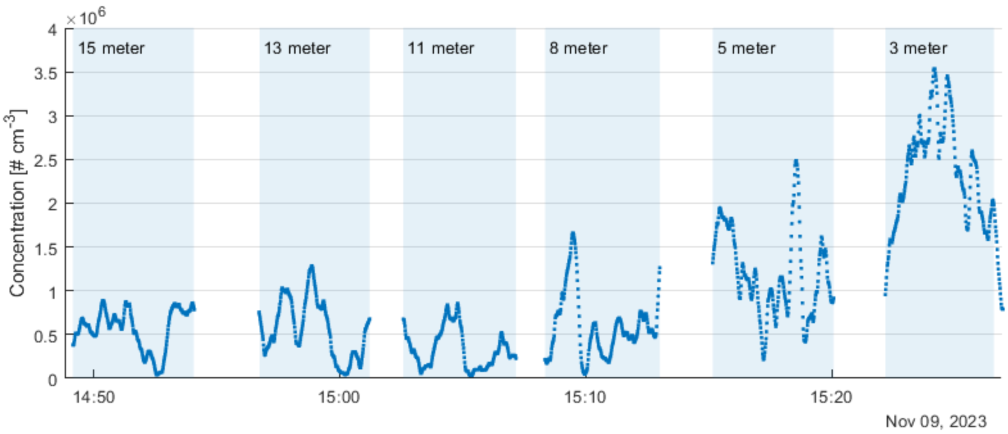

Figure 18: Total UFP concentration (10 - 300 nm) measured by the Naneos Partector 2 over time.

The selected measurement data for each condition is indicated in the plot.

6.3 Main experiment with aircraft & water spray system

This section outlines the test results from the main experiment with all systems in place. First, the evolution over time of relevant quantities are shown. This is followed up by a more in-depth analysis focusing on changes in total particle concentration and LDSA, and finally by an assessment of changes in the particle size (distributions).

6.3.1 Evolution over time

The result of all data cleaning steps (described in Appendix A) is a measurement time window from 2:48 pm till 3:52 pm. This time window includes a background measurement with an *engine off and* a *water spray system off* condition, spanning nearly six minutes, followed by run 1 and run 2. Both runs commence with a baseline measurement with *engine on & water spray system off*, referred to as **40T**, which sets the time for the conditions where the water spray system is switched to "only air", or **40T + A**, and subsequently to "air and water", or **40T + A + W**.

The different conditions are indicated in Figure 19: along with the measured particle concentrations (#/cm^3), both measured by the FMPS and by the Naneos 3[6]. The FMPS particle size range has been set to match the Naneos particle size range: 10 nm till 300 nm. Nonetheless, the Naneos readings are consistently about a factor 2.5 higher than the FMPS readings. This difference could be explained by several factors. Tube losses have not been corrected for, only the dilution factor has been applied on the FMPS concentration results. As discussed in section 5.5, there are losses in the tubes of the FMPS that are more significant for the smaller diameter particles. The Naneos Partector has an accuracy of ±30% within the measurement range (see Table 1), which could lead to a significant under- or overestimation. It should also be noted that the FMPS and the Naneos have different measurement methods, and the Naneos device is not certified for particle concentrations exceeding 1,000,000 (read: a million) #/cm^3. The measured totals get roughly a factor ten higher than this limit. Its behaviour beyond the limit is unknown. However, when comparing the FMPS with the Naneos, the trends over time are highly similar with a Pearson correlation coefficient of 0.93 and 0.95 in run 1 and run 2, respectively.

The measured concentration of UFP particles (at 28 m distance from the engine in the plume) by the FMPS has a mean value of $7.6 \cdot 10^6$ #/cm^3 and $8.3 \cdot 10^6$ #/cm^3 for run 1 and 2 respectively. These values exceed the WHO-recommended 1-hour mean high particle number concentration of 20,000 #/cm^3 by a factor of around 400.

[6] Naneos 3 refers to the Naneos Partector placed downstream of the water screen.

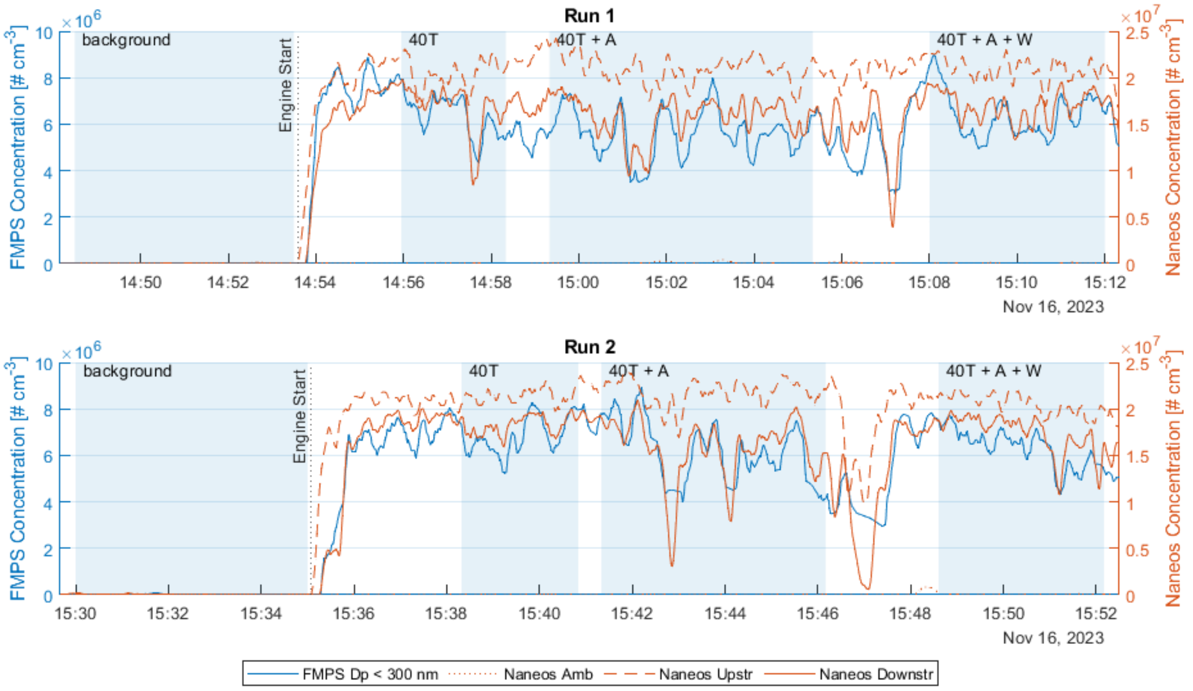

Figure 19: FMPS and Naneos 1, 2, and 3 concentrations (#/cm³) for run 1 and 2 over time (total number of particles 10nm – 300nm).

The selected measurement data for each condition is indicated in the plot. Note the difference in vertical axis scale for the FMPS and the Naneos. Graph colors match the corresponding vertical axis color. "40T" in the figure represents 40% thrust.

Furthermore, Figure 19: shows high fluctuations in particle concentration during the measurements. One explanation for this is the strong correlation with time-variant ambient wind velocities and wind direction. Also, the influence of the water spray system is clearly visible, judged by the fact that the Naneos placed upstream relative to the water spray system shows much less fluctuations than the Naneos (and FMPS) downstream. This can be reasoned by the fact that the water spray system introduces more turbulence to the plume. The particles measured during the background measurements and from Naneos 1 [7] over the entire time span – are hardly visible in Figure 19:, indicating its relative insignificance (<1%) compared to what was measured in the aircraft plume. Note that after turning on the water supply of the water spray system it takes some time for the system to deliver its full capacity. Based on visual observations this took about 30 to 45 seconds.

The effect of windspeed and wind direction on measured concentrations is further elaborated on here. Figure 20: shows a wind rose of the ambient wind and the flow in the plume. The ambient wind and the engine plume have been blowing in opposite directions, causing an increase of concentrations. However, comparing run 1 and run 2 it could be seen that the ambient wind in run

[7] Naneos 1 refers to the Naneos Partector placed at a reference background site near the Citation aircraft yet outside of the plume.

2 turned towards a more perpendicular (or less parallel) direction compared to the plume. The total span in ambient wind direction is in both cases around 45°, ignoring some outliers.

The engine plume was coming from the west-south-west, at an angle of ca. 243°. A clear gap in the wind roses is visible around this angle, indicating the blockage effect of the water spray system. As stated in Appendix A, measurements within 243°±30° are selected to reduce unwanted noise in the measurement data.

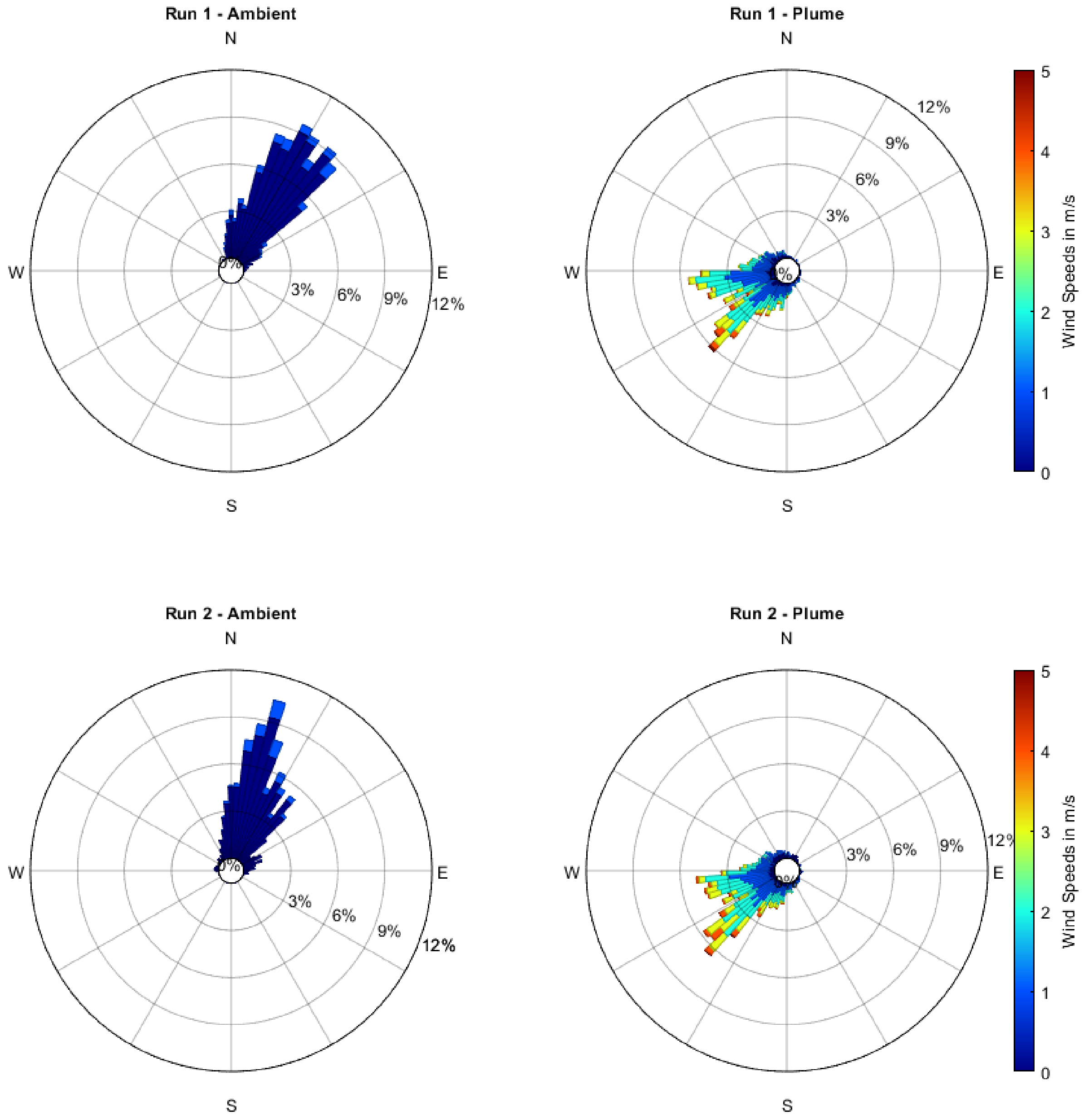

Figure 20: A wind rose for run 1 (upper) and run 2 (lower) of the ambient wind (left) and the wind measured in the plume (right).

The average engine exhaust plume pointed towards WSW (243°).

Flow velocities within the plume were fluctuating between ca. 2 m/s and 6 m/s (at 28 m distance from the engine), whereas the ambient wind speed showed a much smaller fluctuation between ca. 0.5 m/s and 2 m/s. The fluctuations in the plume can mainly be attributed to the turbulence created by the jet engines, as the fluctuations are also visible in the baseline runs where the water spray system was turned off. At the measuring distance of 28 meters from the engine, the momentum of the jet flow has been reduced to such an extent that ambient wind speed had a large influence on the air flow, also attributing to the observed fluctuation in flow velocities (and wind direction).

Besides the conclusions on the effects of the ambient wind and wind direction on the engine plume, the following conclusions can be drawn from the engine thrust setting data, the internal temperature and humidity sensors of the FMPS and Naneos devices:

- Thrust settings are highly constant over time during each operating condition. That shows that the air mass flow from the engine is expected to be constant. Therefore, this parameter is discarded as a potential major influencer of the analysis.
- Both the FMPS and the Naneos are equipped with internal temperature sensors. These measured a much less fluctuating temperature over time than the OIC-406 sensors (ambient temperature and humidity), across all measurement conditions. In case of the Naneos this has been achieved by placing the device casing inlets out of the flow of the jet plume. Within the FMPS, a fan stabilises the temperature.
- Furthermore, the Naneos sampled RH. This parameter was also constant over time, in line with temperature. An average difference of 8% is found between the RH measured downstream compared to upstream in the aircraft plume. Judged by the Naneos and by the strong coupling between temperature and RH, the RH fluctuations within the FMPS are also expected to be minor. The overall RH measured within the Naneos 2 device varied between 64% and 76%, well within the operational limits.
- Based on the OIC-406 measurements, temperature and RH have strongly varied (7°C-16°C for the temperature and 55%-90% for the RH behind the water spray system, driven by measurement condition) within the engine plume. However, the influence of these variations on UFP is not specifically accounted or corrected for as the temperature and RH readings within the measurement devices are stable. Any influence of temperature or RH on the physical properties of the created mist, and/or on the microphysical processes that UFP undergo, are considered a physical effect of the water spray system itself and should not be corrected for within the data processing phase.

Finally, Figure 21: shows the readings of low-cost sensors over time. The CO_2 concentration measurements were not useful for the foreseen purpose of this study, and were therefore omitted from the data. PM_{10}, formaldehyde, volatile organic compound (VOC), and NO_x concentrations are consistently higher on the most centrally located sensors on the frame, where the centre of the frame has been aligned with the radial axis of the plume. Using this information, supported by visual observations of water tracks on the test site and wind socks, it is concluded that the centre of the plume has been captured by the water spray system, as was intended.

In the plots it can be noticed that:

- The background concentrations are the lowest for all sensors.
- At a thrust of 40%, without screen, the PM_{10} concentrations are lower than 40% plus air.
- At a thrust of 40%, with air, the PM_{10} concentrations are lower than 40% plus air and water.
- Sensor 5, the most central sensor, shows consistently higher values than most of the other sensors.

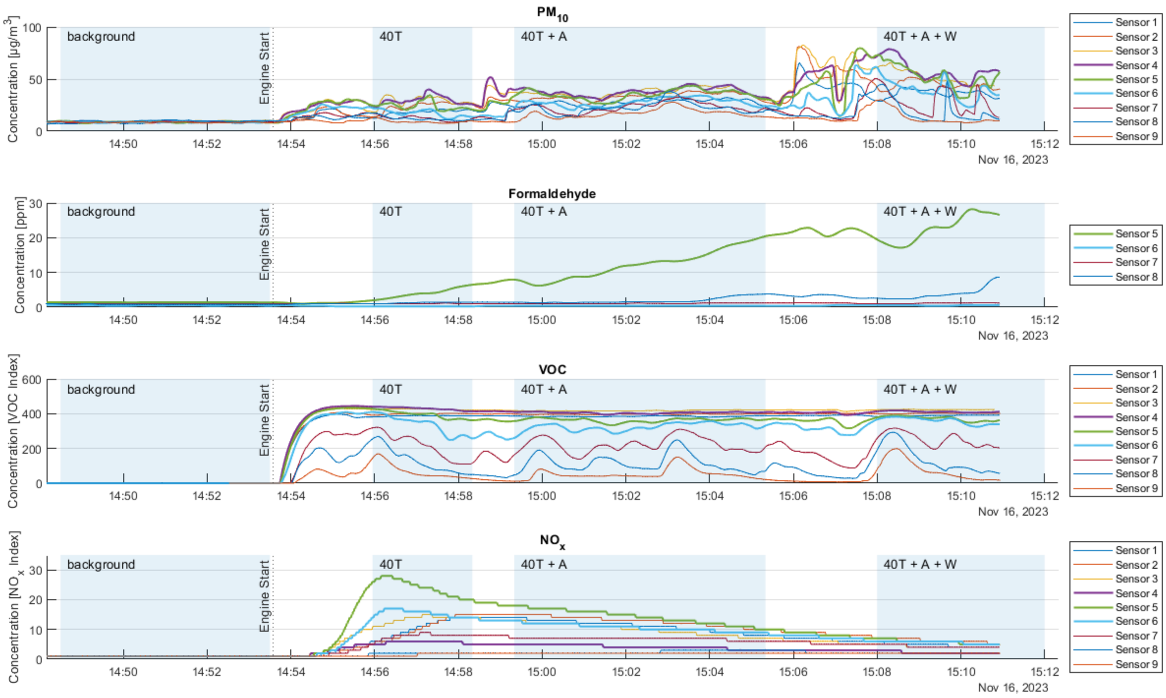

Figure 21: A selection of the low-cost sensors that showed a variation over time.

The three most centrally located sensors are plotted in bold and the selected measurement data for each condition is indicated in the plot. Sensor-numbering from 1 to 9 is from left to right when looking from behind the frame towards the aircraft. “40T” represents the 40% thrust case

6.3.2 Measurement behaviour of the low-cost-sensors

All LCS sensors shown in Figure 21:, showed a reaction when thrust is introduced. The bold lines, representing the sensors placed in the centre of the plume, generally show higher concentrations. The PM_{10}-sensors show high variability over time, and increases when air or water is added to the test.

Formaldehyde sensors show an increase during most part of the test. This could indicate a long settling time at such extreme concentrations. The measurements might not have been long enough for this sensor to fully stabilize, however, the middle sensor (sensor 5) shows higher increases than the other sensors.

The VOC-sensor shows the highest values for the sensors located at number 1 to 5, they also show the least variability over time, as they reached the maximum sensor output of 500 VOC index. The VOC-readings would suggest that the plume was pointed slightly towards sensor 1. However, the background measurements show different off-sets for each sensor, where sensor 1 to 3 show the highest offset, with a difference larger than the difference of the readings between the sensors when thrust was introduced. The datasheet of the sensor also describes a device-to-device variation of up to 15%. The differences are therefore not significant.

The NO_x-sensors show a rapid increase when the thrust is introduced and slowly converges towards zero over time. The NO_x index shows the concentration condition relative to the sensor's history. A NO_x index above 1 shows that the concentration increased with respect to the average concentration over the last 24 hours. As the average concentration increases over time, the increase of concentration decreases over time.

6.3.3 Changes in total particle concentration and LDSA

Figure 22 shows the percentual reductions that have been achieved in terms of the three metrics discussed in Section 5.6. This figure has been created using the PCA analysis combined with clustering as explained in Appendix B, in which the ambient wind conditions and background particle density have been combined into three variables onto which the clustering technique is applied. The percentage difference between the baseline (thrust *on*, water spray system *off*) and the conditions with water spray system also *on* (respectively producing only air, or **A**, and air plus water, or **A + W**) are combined for all clusters into the shown distributions. Cleaned data, from run 1 and run 2 combined, are used.

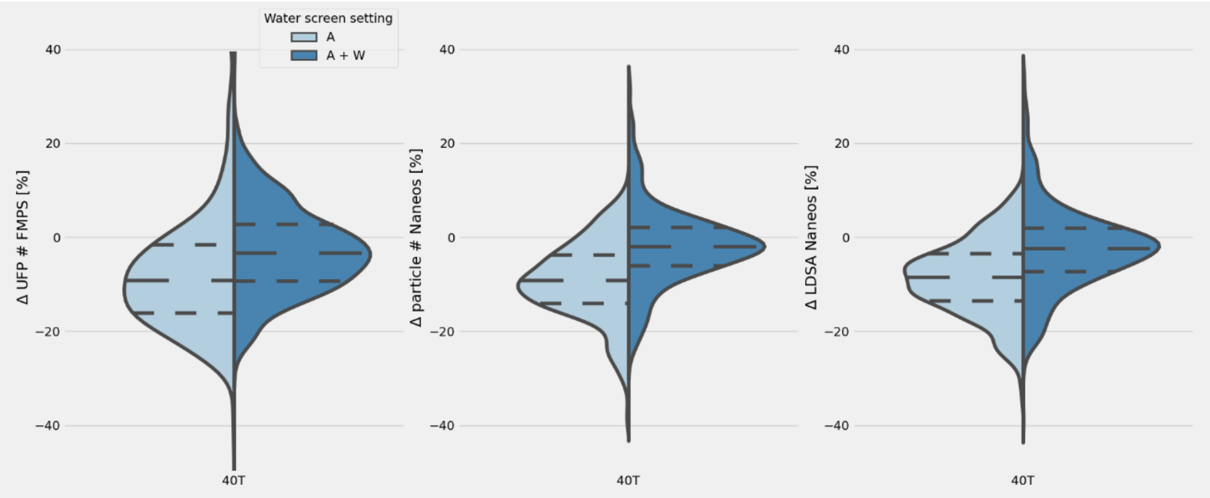

Figure 22: Kernel density estimate (KDE) plots of UFP reductions with a thrust setting of 40%

when the water spray system is on (lighter blue on left side = water spray system blowing air without water, darker blue on right side = water spray system blowing air and water), compared to the baseline where the water spray system is turned off (with the same thrust setting). Dashed lines within the violins show the 25th, 50th and 75th percentile of the values. Left figure shows the change in total particle count from the FMPS within the UFP size range [5.6-100] nm. Middle figure shows the change in total particle count difference between the Naneos that was placed just in front of the water spray system and the Naneos that was placed just behind the water spray system.

A negative quantity in this graph implies a larger reduction in particle count through the plane of the water spray system compared to the baseline. Right figure shows the same as the middle figure, the only difference being that the right figure shows lung-deposited surface area (LDSA) instead of particle count as obtained from two Naneos measurement devices. Data includes measurements during run 1 and run 2 of the experiment combined. The plots show a reduction of UFP for both A as A+W in most, but not all conditions (all values below the zero horizontal indicate a reduction)

For all three metrics, both in the **40T + A** and in the **40T + A + W** conditions, a decrease has been measured compared to the baseline. The focus should be on the comparison between complete utility of the water spray system (**40T + A + W**) and the reference without water spray system (**40T**). However, it cannot remain unstated that in the **40T + A** condition the measured reductions are consistently larger than in the **40T + A + W** condition. This surprising effect could be attributed to different factors, although the exact reason remains unclear. The reduction in **40T + A** is not due to the capturing, coagulation or deposition of UFP in the plume, while **40T + A + W** does have this potential. The spray system introduces more air into the plume which leads to a higher dilution rate compared to the air and water situation. However, the volume of extra air in **40T + A** with respect to **40T + A + W** is expected to be insignificant to the volume of air moved by the engine. Another possible explanation for the lower concentrations could be related to the different interaction of the air with the plume due to the difference in density, this remains to be studied.

Using a *t*-test with a significance level of 0.05, all decreases compared to the baseline resulted to be statistically significant as well as all increases in the **40T + A + W** condition compared to the **40T + A** condition. Note that due to the data cleaning practise, only data on high thrust levels of 40% were left for the analysis.

The main outcomes from Figure 22 are summarized in Table 5, which shows the mean difference between conditions for each metric. This is shown for run 1 separately, run 2 separately, and run 1 and run 2 combined, the latter corresponding to Figure 22. The most important observations from Table 5 are outlined below:

- Particularly when looking at run 1 and run 2 combined, the overall conclusions drawn from the three metrics are consistent and highly similar in magnitude[8].
- When focussing on run 1 and run 2 separately, conclusions are coherent for the Naneos results but not for the FMPS results. For the Naneos downstream of the water spray system, the Naneos upstream could be used over the entire course of the measurement as a reference. For the FMPS there was no reference in-place. The measurement technique of the FMPS and Naneos devices differ substantially, and the measured UFP concentration by far exceeded the upper limit of the certified measurement range for the Naneos. Hence the Naneos does not suffice as a directly comparable reference measurement for the FMPS. With the assumption that both Naneos devices were about equally influenced by

[8] Note that the number of valid measurements within run 1 and run 2 are unequal. Therefore, the reported results of run 1 and run 2 combined are not the average of the reported runs for both runs separately.

the changing meteorological conditions, their (relative) differences are therefore considered as less sensitive to changing ambient conditions in this analysis with the given measurement set-up. This rationale also applies to changing background UFP concentrations, albeit the background concentrations were found to be very small (<1%) compared to the concentrations measured in the plume.

- A consideration of outcomes from both runs is seen as more reliable than a separate evaluation of runs. More spread in ambient conditions will average out the outcomes. The average is more valid for fluctuating environmental conditions. In the future the system could be optimised for the ambient conditions.

Considering all aforementioned and the results from Table 5 leads to the conclusion that particle concentrations and LDSA decrease by 8-9% in the **40T + A** condition compared to the **40T** condition. This decrease is the order of 2-3% in the **40T + A + W** case compared to the **40T** condition. The addition of water (comparison between **40T + A** and **40T + A + W**) increases measured particle number by 6-7%, which could be due to multiple, further to be investigated, factors, e.g. changes in air flow through or around the water spray system, changes in the dilution factor due to different air masses coming out of the screen, coagulation processes taking place in the flow, water droplets itself being measured by the FMPS and Naneos, etc.

Table 5: Difference in a) UFP number count (<100 nm) from the FMPS, b) Naneos total particle count, and c) Naneos LDSA

between a condition with the water spray system turned on and an indicated reference. The results for run 1 and 2 are shown separately, together with the combined runs. The results are based on averaged conditions for each run.

		40T + A vs. **40T**	**40T + A + W** vs. **40T**	**40T + A + W** vs. **40T + A**
FMPS	Run 1	-11.8%	-0.4%	+13.1%
	Run 2	-3.4%	-5.0%	-0.6%
	Run 1 + 2	**-7.5%**	**-2.8%**	**+6.5%**
Naneos particle count	Run 1	-11.0%	-5.8%	+5.0%
	Run 2	-10.2%	+0.2%	+10.3%
	Run 1 + 2	**-9.2%**	**-1.9%**	**+7.1%**
Naneos LDSA	Run 1	-9.9%	-4.2%	+5.6%
	Run 2	-10.6%	-2.5%	+8.0%
	Run 1 + 2	**-8.7%**	**-2.5%**	**+6.2%**

In Figure 23 the difference in particle number between the conditions with water spray system turned on are compared to the **40T** baseline condition, shown as a function of mean ambient head wind, mean ambient cross wind, and wind direction for each individual cluster. This figure illustrates that increases in particle number, when the water spray system is on compared to off **(40T)**, can be related to specific ambient meteorological conditions, mainly when both cross- and head winds are strong (highly negative). This pattern is larger for the Naneos data than the FMPS data. This observation tells that a larger disturbance of the plume flow leads to a less effective (or even negative) decrease of particle density, which can be expected. A strong head wind slows down the plume, which make the plume more inclined to flow around the water spray system, and adds turbulence to the plume which results in improved dispersion. A strong cross wind leads to larger overall lateral deviation of the plume. Overall, the patterns seen from the FMPS and Naneos measurements are very much alike, but the size of the pattern depends on the measurement condition. It can be seen that for the **40T + A + W** condition compared to **40T**, some new regimes of smaller particle density reductions emerge during less disturbing meteorological conditions (less head wind and generally less strong crosswinds).

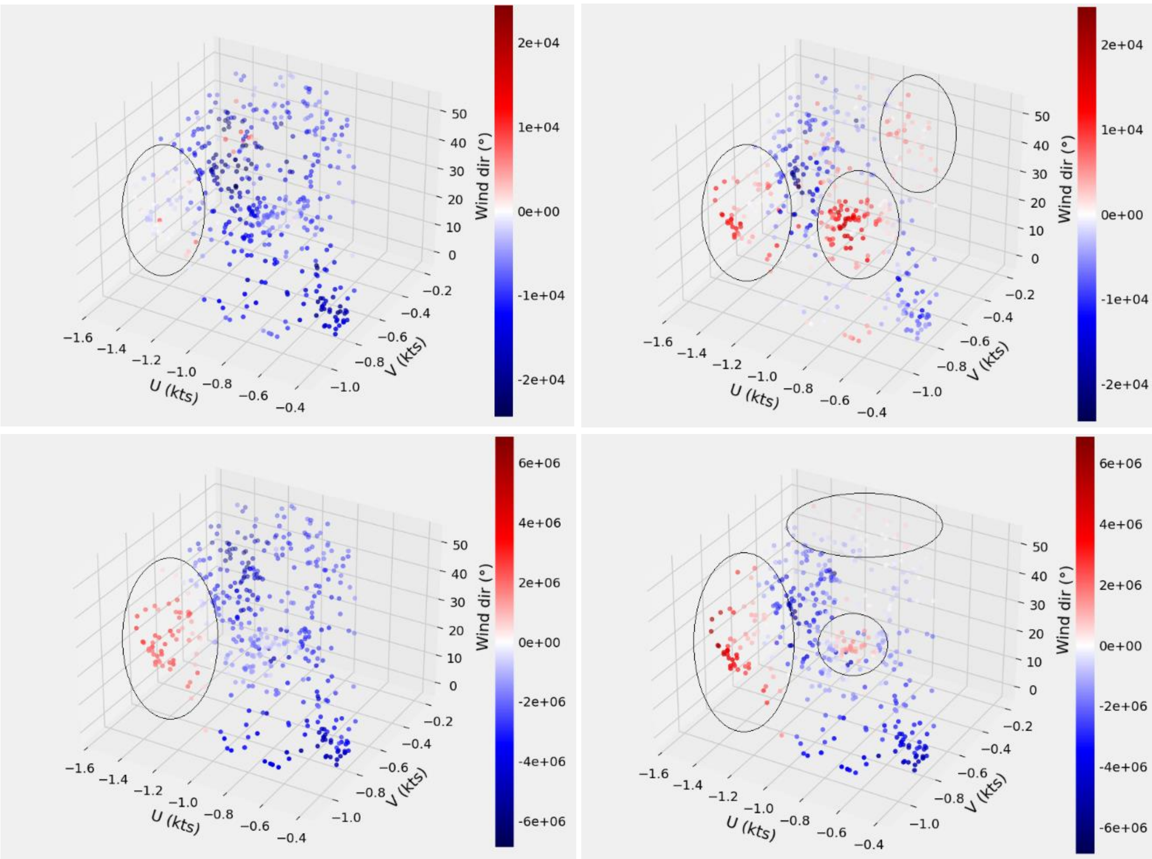

Figure 23: Difference in particle number, represented by the colors.

*between the conditions with water spray system turned on compared to the **40T** baseline condition with the water spray system turned off, shown as a function of ambient head wind (U), ambient cross wind (V), and wind direction (degrees, measured clockwise from the North). Red (blue) color means an increase (decrease) in measured particle density with the water spray system on. Top left: difference in FMPS UFP number count (5.6nm-100nm) for the **40T + A** (only air on) condition. Top right: difference in FMPS UFP number count (5.6nm-100nm) for the **40T + A + W** (air and water on) condition. Bottom left: difference in Naneos particle number count for the **40T + A** (only air on) condition. Bottom right: difference in Naneos particle number count for the **40T + A + W** (air and water on) condition. Note that the measurement range regarding particle size differs between the FMPS and the Naneos. Encircled are the meteorological conditions where particle numbers increase when the water spray system is turned on.*

6.3.4 Changes in particle diameter

The previous section focused on changes in total particle concentration (#/cm^3) and LDSA. This section shifts the focus to changes in particle size: the (aerodynamic) diameter of the particles. Difference in mean particle size amongst measurement conditions are the, not yet discussed, link between the "Naneos particle count" and the "Naneos LDSA" metrics, as discussed in Section

6.3.3. As the penetration of particles within the human body is very much dependent on the size of the particles, and thus associated with health effects, the changes in particle size are worthwhile to zoom in further. The FMPS gives a particle count per bin, which gives a more detailed insight into particle size distributions and changes therein than the Naneos that works with average particle sizes over the entire range based on diffusion.

Figure 24: shows, for each run and each measurement condition separately, the percentage of the total number per particle size in a distribution as measured during the test day. It shows that the major particle size mode is around 10.8 nm, which is in the range of particle sizes that can be measured (with the FMPS) from aircraft engine combustion. Comparing the background (or *zero*) particle measurements to the particle measurements with engine on, Figure 24: shows that the background contains also larger particles than the aircraft plume. In the graph a mode around 30 nm is visible, particularly for the background measurements within the second run. This is possibly due to the air compressor that was coupled to the water spray system, which emitted pollutants through diesel combustion that likely ended up in the plume[9]. The mode at around 30 nm is more clearly visible in the background measurements of run 2 than in run 1, which could be due to changes in wind direction.

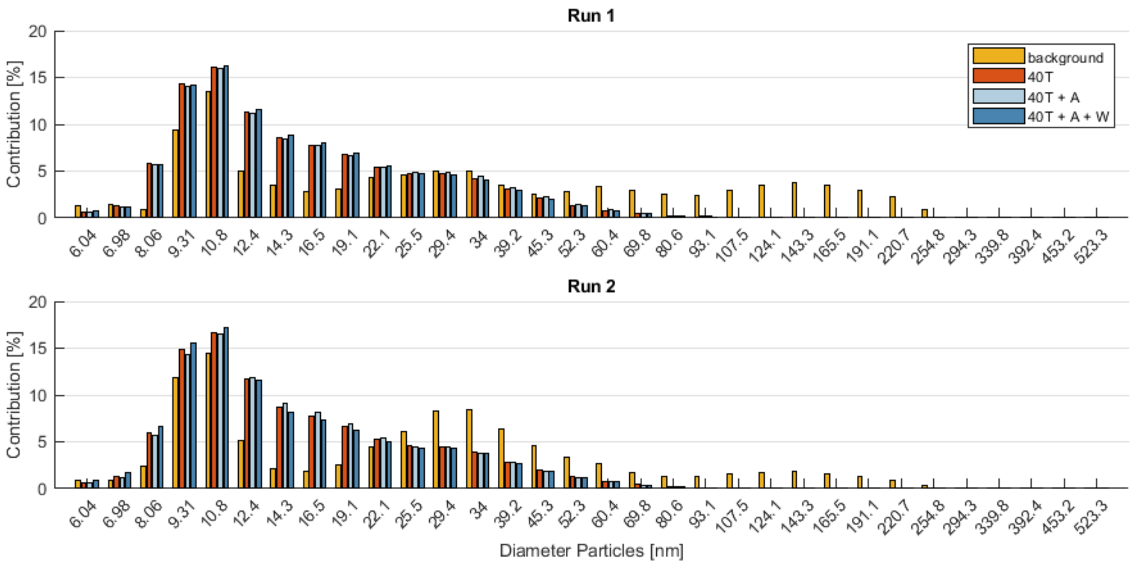

Figure 24: Relative contribution to the total particle concentration over all diameters. Measurement data shown have been extracted from the FMPS.

Whereas overall size distributions and changes therein become apparent, Figure 24: fails to show how particle concentrations *per bin* change in the **40T + A** and **40T + A + W** conditions compared to the **40T** condition, due to the size of the particles observed. This is shown in Figure 25 and **Error! Reference source not found.**Figure 26.

[9] Due to unforeseen wind conditions (wind direction opposite to the exhaust flow) particles from the compressor could have ended up in the measurement section

In addition to the previous observation that larger decreases in particle counts are observed in the **40T + A** condition compared to the **40T + A + W** condition, Figure 25 shows for which particle sizes this occurs. The largest reduction is found for particles of 10 nm, coinciding with the particle size range in which most particles are, as shown in Figure 24. For both conditions there were no absolute differences visible for particles larger (>100nm) than the UFP range. However, the relative difference as shown in Figure 26 clearly shows that an increase of number of particles – larger than ca. 140 nm – is visible when the water spray system is in operating mode, which may relate to a coagulation processes taking place. Furthermore, it is concluded that the addition of water to the plume, with respect to the situation with only air, seems to have no significant, or even a negative impact on measured concentrations for the smallest particles (<29.4 nm in run 1 and <12.4 nm in run 2). A decrease in particle concentration is more pronounced for the particles in the medium size range. This is in contrast with the **40T + A** condition, where particle concentrations appear to decrease stronger for the smallest particles and then again for particles at the edge of the UFP range (100 nm). It should be noted that for this figure no additional filtering or clustering has been done based on meteorological conditions, besides the overall data cleaning procedures. Relative changes in particle count per bin, as shown in Figure 26, expose possible coagulation processes taking place with an operative water spray system, particularly with water, as the particle number tends to decrease below roughly 150 nm and increase above 150 nm.

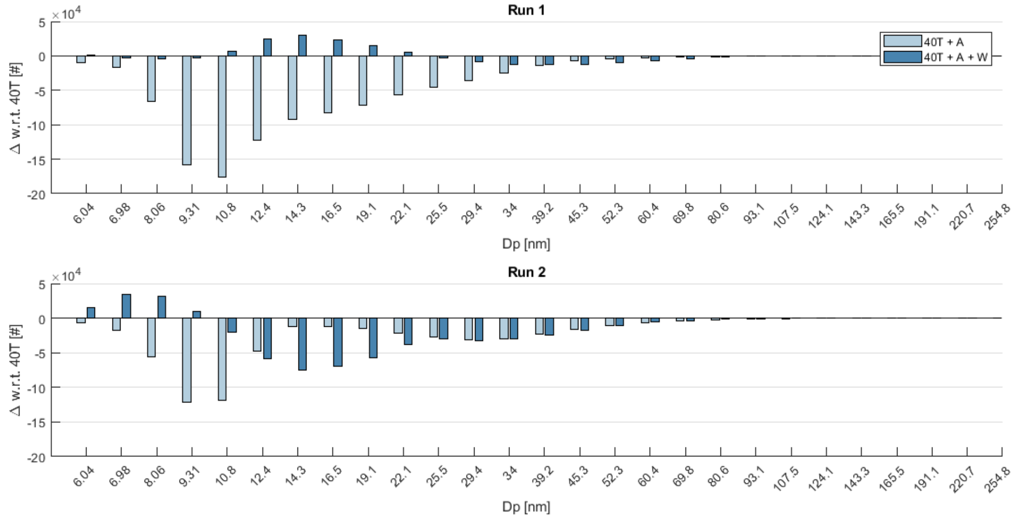

Figure 25: Absolute difference in mean particle concentrations per run and per bin

*in the **40T + A** and **40T + A + W** conditions, compared the condition **40T**, for all bins up to 254.8 nm (FMPS data).*

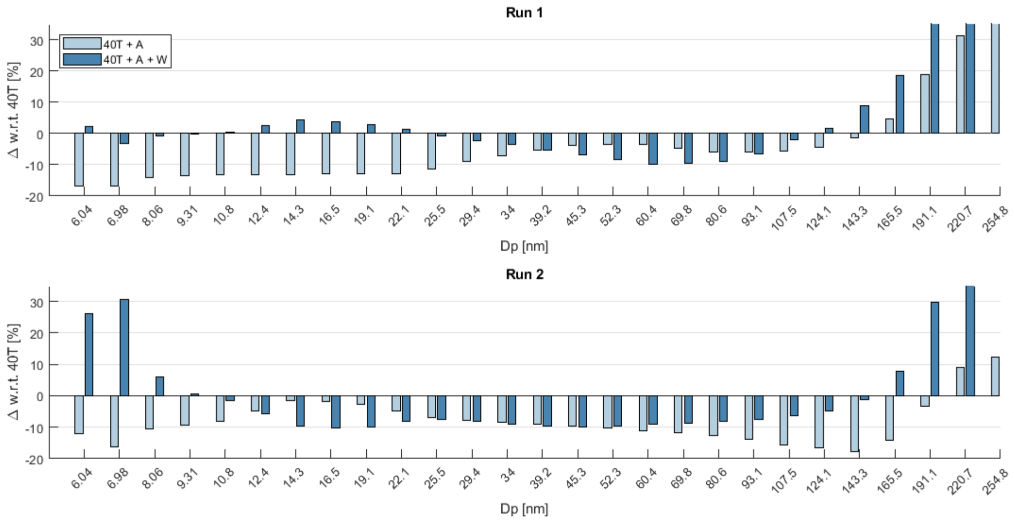

Figure 26: Relative difference in mean particle concentrations per run and per bin

*in the **40T + A** and **40T + A + W** conditions, compared the condition **40T**, for all bins up to 254.8 nm (FMPS data). The particle counts in the larger diameter bins are very low and sometimes zero. The graph therefore shows hundreds of percentages to infinite increases. These are not visualised here and are irrelevant.*

To determine coagulation effects by the spray system on the particles, we calculated the volume-based average particle diameter per second using the data from the FMPS. Coagulation occurs when smaller particles merge to form larger ones. This results in a reduction in the number of smaller particles, and an increase in the number of larger particles. A count-based particle diameter might not effectively capture the coagulation effect, as one large particle could be formed by more than 100,000 smaller particles, making the increase in larger particle counts negligible. Besides, a decrease of particle numbers could be caused by other factors, such as deposition. Focusing on the volume-based approach provides a more clear representation of coagulation because it shows better how the volume shifts over the particle size bins when particles merge. It reduces the dominance of the smaller particles, leading to a more effective analysis of coagulation.

The volume-based average particle diameters are shown in Figure 27:. A variation between ca. 150 and 200 nm is seen during background measurements, for both runs. A sharp drop in average diameter is visible as soon as the aircraft engine was started, decreasing to around 60 to 70 nm. The particle sizes gradually increase again when going from the **40T** to the **40T + A** and finally to the **40T + A + W** condition, each gradual increase being statistically significant as shown by a *t*-test with $\alpha = 0.05$. This suggests that mitigation of smaller particles may take place due to coagulation.

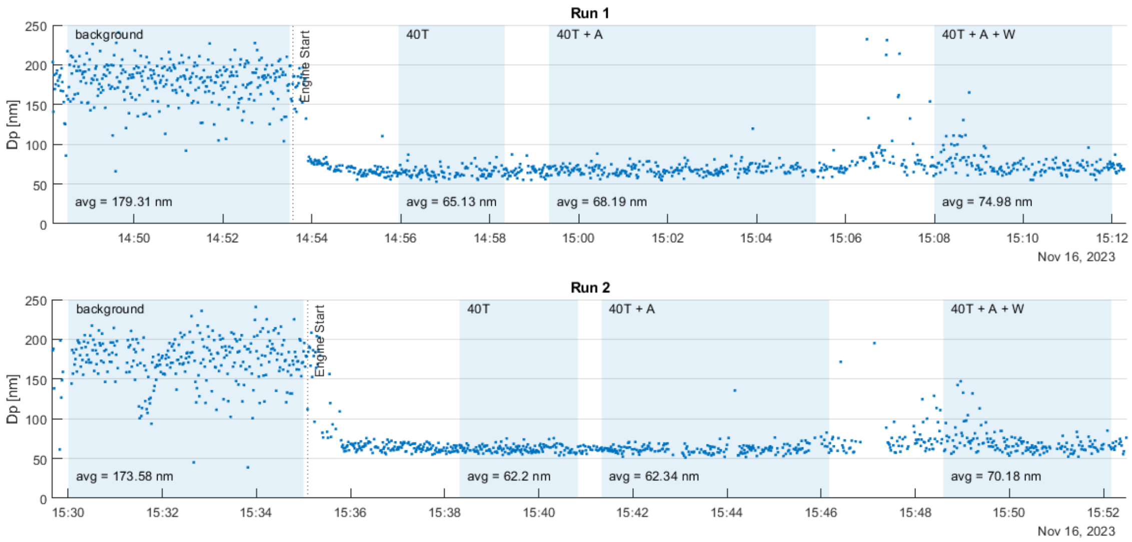

Figure 27: The volume-based average particle diameter, for each timestamp.

The selected measurement data for each condition and average particle diameters are indicated in the plot.

Finally, Figure 28 shows the percentage difference in particle count from the FMPS for all bins separately within the UFP size range [5.6-100] nm, as obtained from the PCA coupled with clustering. It can be seen that this conclusion is in line with the observation in**Error! Reference source not found.** for UFP of ca. 40 nm and larger, the percentage reduction with respect to the baseline is larger in the **40T + A + W** condition than in the **40T + A** condition. Below 40 nm, where most particles are, in the **40T + A** condition the relative reduction with respect to the baseline is larger than the one in the **40T + A + W** condition. This means that compared to air blowing, water is found more effective in reducing UFP that are larger than ca. 40 nm while air (without water) is found to be more effective in reducing the smallest UFP that are being produced by the aircraft engine. The earlier reported stronger overall decrease of the particle concentration in the **40T + A** condition compared to the **40T + A + W** condition, also follows from Figure 28; most particles are found in the particles size range from ca. 9 to 15 nm (see Figure 24:). The decreases of particle concentrations are larger for these particle sizes in the **40T + A** condition than in the **40T + A + W** condition. Figure 28 does not give further information on the observed increase in average particle size in the **40T + A + W** condition (compared to the **40T** and the **40T + A** condition).

Combining all results, the UFP particles between ca. 30 nm and 100 nm seem to coagulate to particles larger than the UFP range (>100 nm) under the influence of water droplets. The data gives no indication that these water droplets have been effective in mitigating the smallest particles that reside from the aircraft engine (10-20 nm). Yet, the results may (partially) be an artefact of local changes in air flow that are being caused by different water spray system settings. This should be investigated further. Also, auto-ionisation of particles may help in capturing particularly the smallest particles, as will be elaborated on in Chapter **Error! Reference source not found.**.

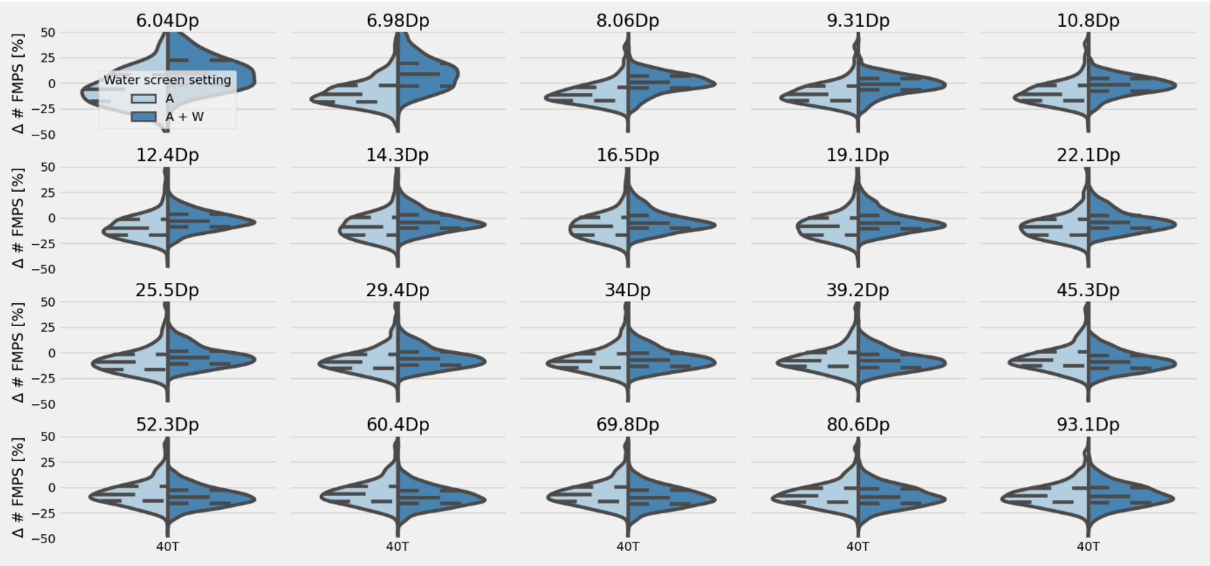

Figure 28: Kernel density estimate (KDE) plots

showing the percentage difference in particle count from the FMPS for all bins separately within the UFP size range [5.6-100] nm. The average bin size diameter is shown in the caption above each subplot.

6.3.5 Deviations from the designed experiment

Due to weather conditions, the aircraft was not able to arrive on the planned arrival time. Therefore, the test matrix was narrowed down. The time that was left did not allow for varying the distances of the water screen and sensors in the test setup or repetitions of the runs to minimize the uncertainties.

The average and expected (and preferred) wind direction at the airport was south-western wind, however, north-eastern wind occurred on the day of the experiment. The test setup was designed to have the aircraft nose pointing into the wind, so that the measurements would take place downwind of the emission source. The test location did not have sufficient space to allow for rotating the test setup, leading to a setup where the aircraft nose was pointed away from the wind. Due to the wind being in the opposite direction, no measurements were done while the water spray system was operative without aircraft engine as the mist drifted away from the sensors.

6.4 Main conclusions experiment result and recommendations for future experiments

6.4.1 Main conclusions on experiment results

The results indicate an effect of the water spray system on the amount and particle size of the UFP concentration from the aircraft engine but not to the extent that was desired (15% reduction).

- Ultrafine particle concentrations and the calculated lung-deposited surface area show a statistically significant decrease when the designed water spray system is in operative mode compared to an inoperative screen. This effect (8-9%) is larger for the condition in which the screen only ejects air than when water is used (2-3%). Particles in the range of 10 to 20 nm, the dominant particle size for aircraft emissions, showed inconclusive results across different runs.
- A reduction of UFP concentration was measured in the range of ca. 30 nm and 100 nm when the water spray system was operative, while an increase was measured of particles above ca. 150 nm. In the aircraft plume the measured average particle diameters are in the order of 62-65 nm. This shifts to 70-75 nm when the water spray system is ejecting water droplets into the plume. These results are consistent across different runs. Altogether, the data suggests that coagulation takes place under the influence of the water spray system.
- The UFP measurement outcomes were very sensitive to the changing ambient conditions. During the main experiment wind speeds were very low (mostly ~0.5 m/s with peaks of 2 m/s), yet the wind direction was highly volatile up to the point that ambient wind was opposite to the exhaust plume. Based on expert judgement, ambient wind direction was identified as one of the key parameters in the experiment. Due to a limited time and space at the test site it was not possible to rotate the aircraft or equipment or wait for more favourable environmental conditions. In academic sense this leads to the conclusion that, with the presented experiment set-up, no clear conclusive statements about the UFP reduction potential of the water spray system could be made. In practical sense, the sensitivity to environmental conditions of the setup as tested provide challenges for the implementation in an operational airport environment. Due to this sensitivity in combination with lower than anticipated reduction in UFP we conclude that mitigation with the water spray system demonstrated in WP7.1 is not operational feasible.

6.4.2 Recommendations for future experiments

Whilst the experiments were designed with care and taking into account a large body of knowledge from literature (as described in section 4) and a previous smaller-scale droplet screen experiment at Amsterdam Airport Schiphol (described in section 3.2), the exploratory nature of science led to a few new insights, surprising findings and recommendations to improve on for additional experiments out of cope of TULIPS WP7.1.

- A question that remains inconclusive, is to what extent the observed decreases in particle concentrations can be attributed to a decrease in airborne UFP. The effect of dilution, which is inevitably the case whenever a volume of air is added to the flow through the water spray system, has played a role and could yet not be accurately quantified for the performed experiments. Furthermore, disturbance of the plume by the water spray system has led to changes in turbulence and flow patterns which are hard to quantify when measuring at one specific location behind the water spray system. It is therefore recommended to perform measurements on multiple positions behind the water spray system, and to improve on visualisation of flow patterns and disturbances.
- It is well known that other emission sources can pollute measurement data. For this reason auxiliary equipment such as the pumps and compressors were placed downstream of the measurement equipment. However, due to the unexpectedly changing wind direction, particles with a size signature matching the compressor were found in the measurement data. It is therefore recommended to take this into account and to take preventive measures to prevent pollution in deviating conditions.
- The abovementioned contamination was detected by comparing readings from multiple, inter-calibrated sensors of the same type, in this case the Naneos-sensors. It is therefore recommended to include duplicates of the most vital sensors. Due to cost and limited availability it was not feasible to include a second FMPS in the experiment, but doing so would have helped draw more general conclusions under the volatile environmental conditions that were encountered.
- As the estimated tube losses calculated by Baron and Willeke (2001) show that significant losses are possible, especially for smaller UFP particles. It is recommended to include a measurement of the concentrations without tubing to determine the actual losses in the used test setup. As it is not expected to change the outcome of the analysis, it would help understanding the correlation between the FMPS and the Naneos. Furthermore, it would give a more realistic representation of the actual UFP concentrations behind an aircraft engine.

The effectiveness of the water system in the setup that was tested proved less effective than anticipated. Mathai (1984) and Hassler (1978) have shown that ionisation of water droplets can have a large impact on particle capture efficiencies. Whilst active ionisation by applying an electric charge to the droplets was deemed a safety risk, passive charging by grounding the water system might provide a safe alternative worth investigating. Given time constraints it was not possible to pursue this further on the test location of the main experiment. In the study from Hassler (1978) de-ionised water has been charged by means of the friction of water along the metal in the nozzle, referred to as autogenous charging. Autogenous charging is effective when the nozzle system is *directly* connected to the ground, so that no charge build-up can take place. The use of deminiralised water (as used in the main experiment) would complement a grounded setup.

7 Conclusion and recommendations

7.1 Conclusion

Our results indicate that using a water spray system to mitigate UFP, influences the amount and particle size of the UFP concentration from the aircraft engine. However, not to the extent that was desired (15% reduction). We conclude that mitigation with the water spray system demonstrated in WP7.1 is not operational feasible due to the complexity of UFP and the mitigation set-up.

Our study has revealed numerous uncertainties regarding the behaviour and influences of ultrafine particles (UFPs). While existing research has provided some valuable insights, there remains a substantial amount of unforeseen factors, representing a critical blind spot in our knowledge. Numerous variables impact UFP and its behaviour, yet their precise effects are still not clearly understood. This complexity underscores a significant gap in our comprehension, especially concerning the real-world operational environment of an airport. This lack of detailed insight may have significantly influenced the results of our experiments, further investigation is needed to fully understand the most influential factors at play and their potential implications before acting on the mitigation of UFP.

7.2 Recommendations

We recommend discontinuing testing the mitigation strategy using a water spray system. Given the complexity of the issue, the approach is not economically scalable and the demonstrator did not achieve the desired mitigation effect. However, it has deepened our understanding of UFP behaviour and highlighted the importance of continuous measurement and gaining new insights in potential alternative mitigation strategies, which will guide our future efforts towards effective UFP mitigation at Amsterdam Schiphol Airport.

To develop successful mitigation strategies and understand their deployment, it is essential to first comprehensively collect the data current UFP situation and observe the behaviour and influential factors within the airport operations.

The logistical and technical aspects of the continuous measurements should be prioritized, and the details will be covered in Deliverable 7.3. We recommend to first build a Minimum Viable Product (MVP) to assess the feasibility of effectively mapping UFPs and accurately tracking our experiments. We propose a year-long measurement period to account for seasonal variations, ensuring a robust dataset that will inform our approach to UFP management.

By concentrating on continuous measurement and detailed data analysis, we aim to uncover the nuances of UFP behaviour and develop informed strategies for effective mitigation. This approach will enable us to address the complexities and challenges identified in our experiments, ultimately leading to improved air quality management at the airport.

References

Andronache, C., Grönholm, T., Laakso, L., Phillips, V., & Venäläinen, A. (2006). Scavenging of ultrafine particles by rainfall at a boreal site: observations and model estimations. *Atmospheric chemistry and physics*, 4739-4754.

Baron, P. A. (2001). Aerosol measurement: principles, techniques, and applications. . In P. A. Baron, *Aerosol measurement: principles, techniques, and applications.* John Wiley & Sons.

Chapman, P., Clinton, J., Kerber, R., Khabaza, T., Reinartz, T., Shearer, C., & Wirth, R. (2000). CRISP-DM 1.0: Step-by-step data mining guide.

Hassler, H. A. (1978). A new method for dust separation using autogenous electrically charged fog. *Journal of Power and Bulk Solids Technology, 2*, 10-14.

Janssen, N., Houthuijs, D., & Dusseldorp, A. (2022). *Gezondheidseffecten van ultrafijn stof van vliegverkeer rond Schiphol.* Bilthoven, The Netherlands: RIVM.

Jolliffe, I., & Cadima, J. (2016). Principal component analysis: a review and recent developments. *Royal Society, 374*(2065). doi:https://doi.org/10.1098/rsta.2015.0202

Kulkarni, P. B. (2011). *Aerosol measurement: principles, techniques, and applications.* John Wiley & Sons.

Mathai, C. (1984). *A new charged fog generator for inhalable particle control.* Washington DC, USA: US Environmental Protection Agency.

Møller, K., Brauer, C., Mikkelsen, S., Bonde, J., Loft, S., Helweg-Larsen, K., & Thygesen, L. (2020). Cardiovacular disease and long-term occupational exposure to ultrafine particles: a cohort study of airport workers. *International Journal of Hygiene and Environmental Health*, 214-219.

S. Kojevnikova, Y. Z. (2000). Mechanism of Collection of Aerosols by an Array of Opositely Charged Drops. *Journal of Aerosol Science*, 437-461.

Sobczyk, A., Jaworek, A., Marchewicz, A., Krupa, A., & Czech, T. (2019). Particulate matter emission reduction from marine diesel engines by electrhydrodynamic methods. *KONES Powertrain and Transport*, 203-210.

TSI. (n.d.). *Ultrafine Particles in Ambient Air*. Retrieved from TSI: https://tsi.com/resources/ufp-monitoring-fundamentals-and-more/

Viitanen, A. K. (2017). Workplace measurements of ultrafine particles—a literature review. *Annals of Work Exposures and Health*, 749-758.

Appendix A: DATA PROCESSING USING CRISP-DM

The CRoss-Industry Standard Process for Data Mining (CRISP-DM), see Figure 29, is used as a framework within the data mining process, aimed at the extraction of valuable information from the large data pool obtained from the main experiment. This section aims at giving a brief overview of the relevant aspects within this study regarding data processing, seen as steps of the *data understanding* and *data preparation* phases. The modelling approach is further described in Appendix B.

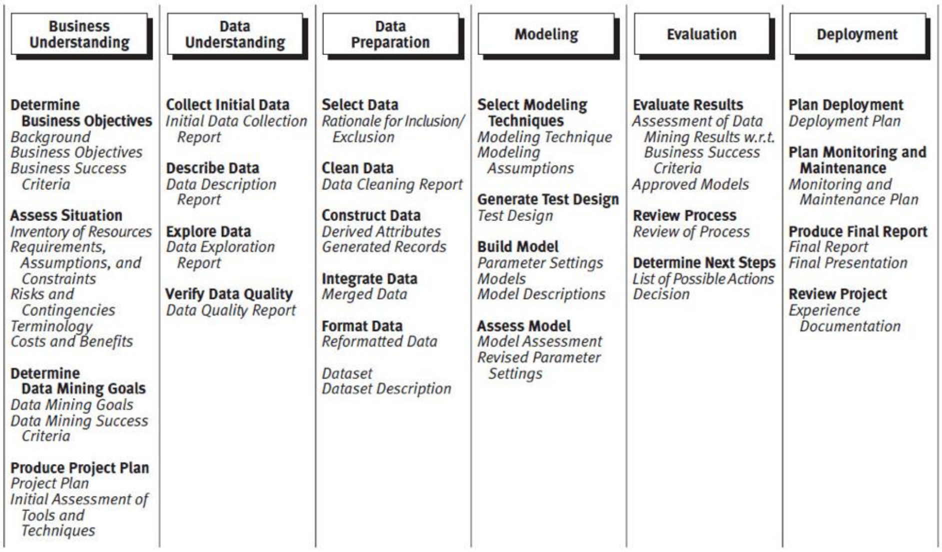

Figure 29: CRISP-DM phases and related tasks. Extracted from Chapman et al. (2000).

7.3 Data Understanding

All CRISP-DM procedures regarding data understanding, as indicated in Figure 29, have been executed. Upon collection and exploration of the data sources, some malfunctioning had been detected for either the hardware or software related to the low cost sensors within the aircraft plume, which lead to missing data from run 2 onwards. Similarly, no footage has been extracted from the GoPro-2 (located upstream) within run 3. For all other data sources, data had been continuously collected over the entire course of the test day, as shown in Table 6.

Table 6: Data collection. Whenever a data source has successfully measured and logged during a particular run, this has been indicated by a cross (x).

Sensor	Location	Run 1	Run 2	Run 3
FMPS	Downstream	x	x	x
Naneos-1	Ambient	x	x	x
Naneos-2	Upstream	x	x	x
Naneos-3	Downstream	x	x	x

Meteo-1	Ambient	x	x	x
Meteo-2	Downstream	x	x	x
LCS-1	Ambient	x	x	x
LCS-2	Downstream	x		
GoPro-1	Ambient	x	x	x
GoPro-2	Upstream	x	x	
GoPro-3	Upstream	x	x	x
Citation	Left engine	x	x	x

7.4 Data Preparation

The data preparation steps are structured according to the *data preparation* phase described in CRISP-DM, which includes 1) data selection, 2) data cleaning, 3) data construction, 4) data integration, and 5) data formatting (Chapman, et al., 2000). These steps are discussed below.

7.4.1 Select Data

An overview of the selected parameters as collected from the FMPS, Naneos devices, the Windmasters, and the OIC-406 sensors is shown in Table 7. The internal temperature and humidity readings of the FMPS and Naneos are used to check whether the sensors remain within their operating windows to ensure their correct functioning. For the FMPS, the particle count per bin[10] has been selected for the analysis, along with the internal temperature measurement. The particle count from the Naneos devices is selected, as well as the lung-deposited surface area (LDSA) for the Naneos devices within the plume. Within the Naneos devices the internal temperature and relative humidity measurements were used to check whether these quantities remain relatively constant and well within operational limits to detect possible malfunctioning. The Windmaster outside of the aircraft plume is used for the monitoring of (changes in) ambient wind conditions, while the wind direction measured in the plume is used to filter the data on, as will be elaborated on below. The OIC-406 sensor on the background site is used to check whether ambient temperature and relative humidity has remained relatively constant during the measurement campaign, while the plume-impinged OIC-406 sensor is used 1) as an additional tracer for the various measurement conditions (engine on/off, water spray system on/off) and 2) to define when the measurement conditions reach (quasi) steady state after switching from one condition to the other.

[10] The FMPS measurement sensitivity ranges from 5.6nm to 560nm particles, with a total of 32 channels or bins in which the particle count is assessed. These bins are centred at 6.04, 6,98, 8.06, 9.31, 10.8, 12.4, 14.3, 16.5, 19.1, 22.1, 25.5, 29.4, 34, 39.2, 45.3, 52.3, 60.4, 69.8, 80.6, 93.1, 107.5, 124.1, 143.3, 165.5, 191.1, 220.7, 254.8, 294.3, 339.8, 392.4, 453.2, and 523.3 nm.

Table 7: Selected parameters from each measurement device (excluding low-cost sensors).

	FMPS	***Naneos*** *background*	***Naneos*** *upwind screen*	***Naneos*** *downwind screen*	***Windmaster*** *background*	***Windmaster*** *plume*	**OIC-406** *background*	**OIC-406** *plume*
Particle count	X (in bins, till 100nm)	X	X	X				
Lung Deposited Surface Area			X	X				
Temperature	X	X	X	X			X	X
Particle volume	X (in bins)							
Relative humidity		X	X	X			X	X
Total wind speed					X			
North-South wind speed					X			
West-East wind speed					X			
Wind direction					X	X		

It should be noted that the FMPS and Naneos devices also calculated particle mass. These records have not been analysed as it is not within the scope of this study. Furthermore, the low-cost sensors yield data on CO_2, NO_x, formaldehyde, and particulate matter concentrations.

7.4.2 Clean Data

With the selected parameters, an effort was made to remove unreliable or missing data. The data cleaning process exists of the following steps:

- removal of records with any missing data. Whenever a record does contain any missing values – whether it being one of the FMPS, Naneos or meteorological measurements – does contain any missing values, the second in which this takes place is omitted entirely;
- all 46 records where the meteorological measurement quality flag is zero ("low") were removed;
- some records containing invalid FMPS or Naneos data were removed:
  - short time windows (order of minutes) just after the change of measurement conditions – being combinations of thrust settings and water spray system settings – were omitted to account for "settling" time. External temperature and relative humidity measurements have been combined with expert judgement to determine the most applicable time window in which the quantities reach (quasi) steady state;
  - during changes in conditions (switching on air/water and other interruptions in the test area, based on GoPro's or notes);

  - measurements with unlikely/unexplained low or high concentrations (outliers);
- run 3 is removed entirely from the data since the ambient meteorology changed drastically during this run, compromising the use of the baseline (reference) measurements;
- measurements where the wind direction in the plume was outside of the 243°±30° range have been omitted to reduce unwanted noise in the measurement data.

After all aforementioned data cleaning steps, roughly 1,800 complete records (cumulatively 30 minutes) of data remained for further analysis.

7.4.3 Construct Data

The construction of new data features has been applied to aid the analysis and answer the research questions with higher confidence. It included the following:

- Decomposition and subsequent summation of the original North-South and West-East wind components, measured by the Windmasters, into:
  - a wind component projected on the direction parallel to the aircraft plume, from now on called *head wind*, and;
  - a wind component projected on the direction perpendicular to the aircraft plume, from now on called *cross wind*.

  This decomposition aids the interpretation of the influence of various wind components on measured particle densities.
- Definition of the water spray system setting and thrust setting of the aircraft, based on time-stamped logs and the logging of the thrust settings. Calibration of this logging has been done by comparing the thrust setting data with particle count measurements. By this means the data can be categorized into different measured conditions, being:
  - a baseline with the engine on 40% thrust while the water spray system was off, referred to as "**40T"**;
  - a condition in which the water spray system was switched to ejecting air, while the aircraft engine was still producing 40% thrust, referred to as "**40T + A"**;
  - a final condition in which the water spray system was switched to ejecting water and air, while the aircraft engine produced 40% thrust, referred to as "**40T + A + W"** .

7.4.4 Integrate & Format Data

The integration of all different data sources requires synchronizing the time stamps of the various data. Two out of three Naneos devices were corrected by an hour to convert to UTC time. The low-cost sensors in the plume were corrected by 5 seconds to correct for the small mismatch with GPS time. Furthermore, 7 seconds were subtracted from FMPS measurement times to correct for the travel time of air through the inlet. FMPS and Naneos measurement were put side-by-side and necessary timestamp corrections were applied so that peak concentrations overlapped (order of seconds). Before merging, care was been taken that all data sources were downsampled onto a time resolution of 1 second.

Appendix B: PRINCIPAL COMPONENT ANALYSIS COMBINED WITH CLUSTERING

As has been discussed in Section 5.6, the variations over time of wind conditions and background particle density are accounted for in the analysis by a technique combining Principal Component Analysis (PCA) and clustering. PCA takes the covariance of an original set of parameters into account and creates a new subset of parameters (Principal Components, from now on referred to as PCs) that are a linear combination of the original parameters, such that most of the variance that was contained in the original parameters is captured (Jolliffe & Cadima, 2016). The ultimate goal of this is to reduce the dimensionality of the original data, combining parameters which are highly collinear and preserving as much information as possible that is contained within the data. For the sake of this study, the following measured parameters are considered within the PCA, based on expert judgment:

- ambient wind speed;
    - ambient head wind;
    - ambient cross wind;
    - total ambient wind speed;
- ambient wind direction;
- UFP background concentrations.

These parameters are external factors that vary independently of any changes invoked by either the aircraft engine or the water spray system. As can be seen from Figure 30, some of these parameters co-vary.

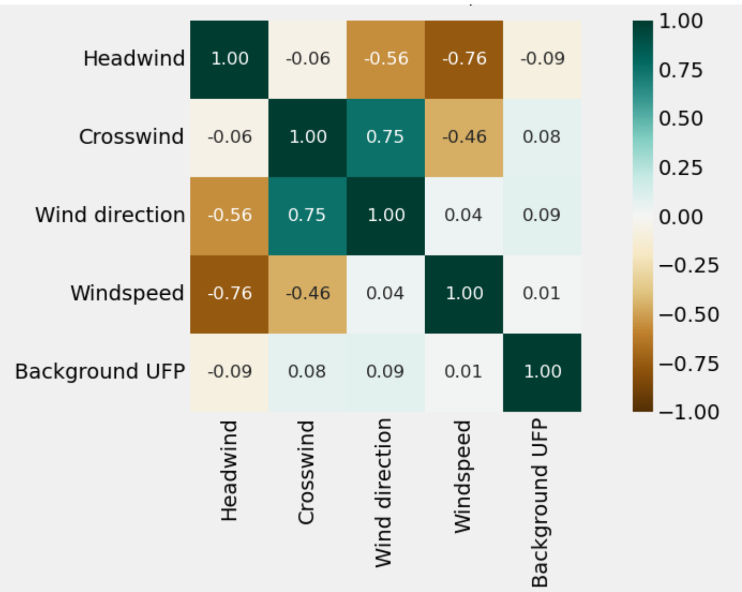

Figure 30: Pearson's correlation coefficients between disturbing factors.

Headwind, cross wind, wind direction and wind speed are taken from Windmaster measurements; background particle number is derived from Naneos measurements continuously outside of the aircraft plume.

Figure 31 shows which percentage of the original variables' variance is captured by the PCs as a function of the number of PCs chosen. As a rule of thumb the PCs should collectively contain at least 80% of the original variance, which is the case from 3 PCs in this case[11].

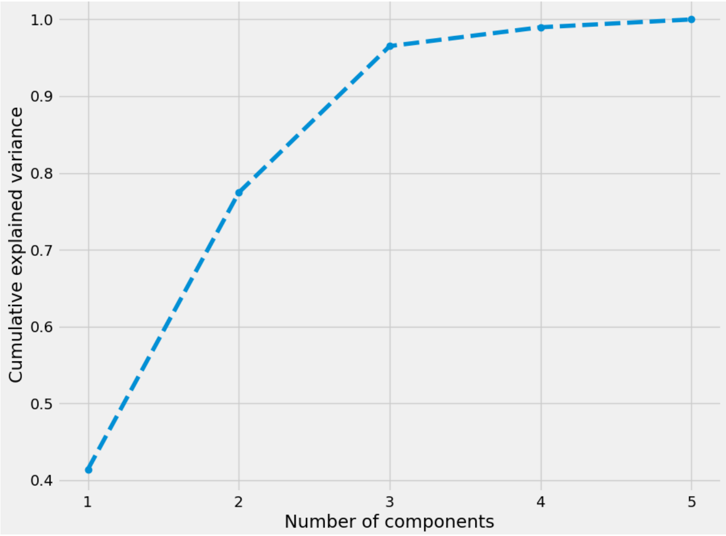

Figure 31: The total variance captured by the principal components (PCs)

plotted as a function of the number of principal components (sorted in decreasing order of explained variance).

Finally, Figure 32 shows how the original parameters work their way through the set of 3 newly created parameters, or PCs. As could also be seen from Figure 32, head wind and wind speed are highly anti-correlated and dominate PC 1, while cross wind and wind directions are highly anti-correlated and dominate PC 2. Background particle concentration show low covariance with the other parameters and solely dominate PC 3. This is all in line with Figure 30.

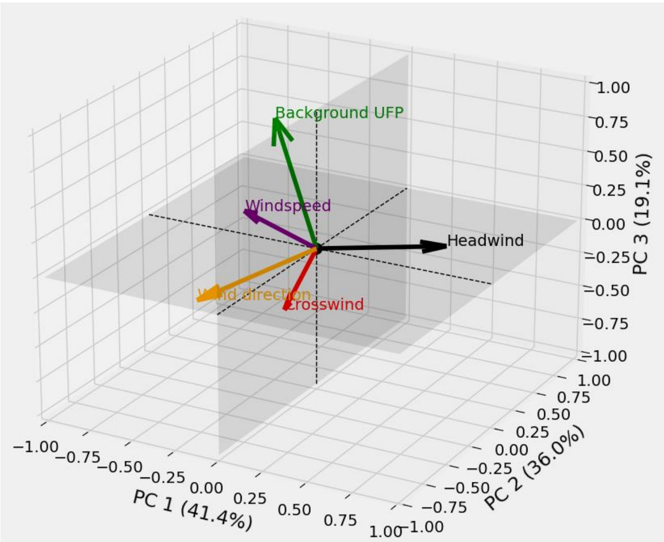

Figure 32: Loading plot showing the contributions of the original ambient meteorological parameters in the newly created principal components.

[11] 96% of the variance is contained within the first three principal components.

All data points[12] (ca. 1,800, or 30 minutes cumulatively) are then clustered based on similar values for the newly created PCs, leading to subsets of measurements which have all been measured within similar ambient conditions. Each cluster may contain different measurement conditions (i.e. combinations of thrust setting and water spray system settings) amongst which the measured particle concentrations could be directly compared to each other. This leads to a more fair comparison between measurement conditions, as the ambient conditions within the cluster of measurements have been similar. This method is illustrated in Figure 33 for two randomly chosen clusters.

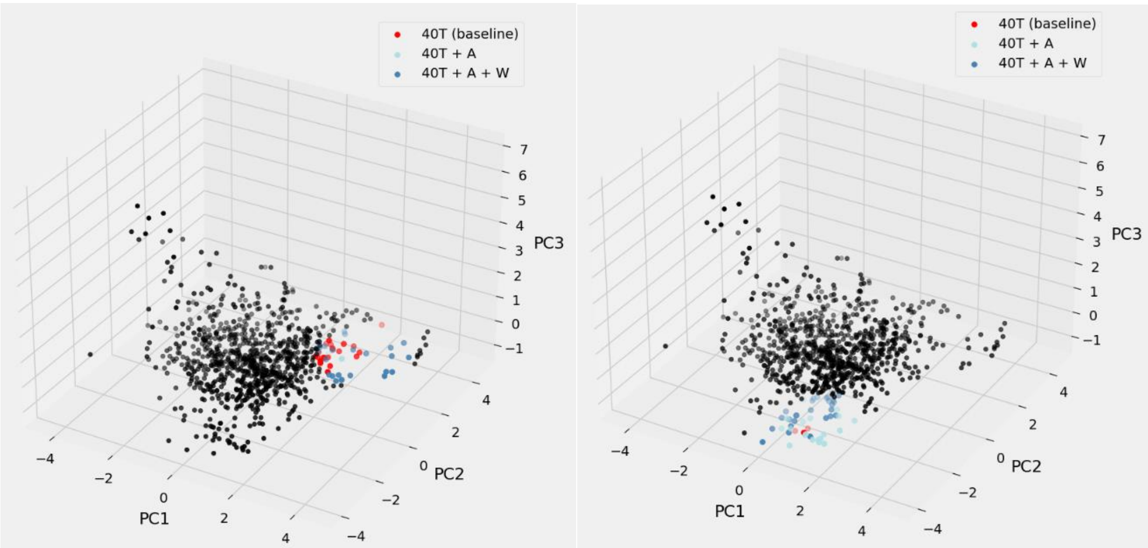

Figure 33: Clustering methodology illustrated in two examples for two different clusters found in the dataset.

The axes correspond to the three selected principal components that altogether explain about 96% of the original variables' variance.

[12] A data point is a single second in which measurements from the FMPS, Naneos and Windmaster devices have been extracted and which passed all data cleaning procedures.